

Traçage isotopique



Table des matières

Chapitre 4: Traçage isotopique	139
A. Article "Isotope tracing of atmospheric mercury sources in an urban area of northeastern France"	141
A.1. Abstract	141
A.2. Introduction	141
A.1. Materials and Methods	141
A.2. Results and Discussion	142
A.1. Literature Cited	145
A.2. Supporting information	147
B. Article "Tracing and quantifying anthropogenic mercury sources in soils of northern France using isotopic signatures"	169
B.1. Abstract	169
B.2. Introduction	169
B.3. Materials and Methods	170
B.4. Results and Discussion	171
B.5. Literature Cited	175
B.6. Supporting Information	177

Isotope Tracing of Atmospheric Mercury Sources in an Urban Area of Northeastern France

NICOLAS ESTRADE,^{*,†,‡}
JEAN CARIGNAN,[†] AND
OLIVIER F. X. DONARD[‡]

Centre de Recherches Pétrographiques et Géochimiques (CRPG), Nancy-Université, CNRS/INSU, 15 rue Notre-Dame-des-Pauvres B.P. 20 F-54501 Vandœuvre-lès-Nancy, and Institut Pluridisciplinaire de Recherche sur l'Environnement et les Matériaux, Laboratoire de Chimie-Analytique Bio-Inorganique et Environnement, Université de Pau et des Pays de l'Adour, CNRS UMR 5254, HELIOPARC, 64053 Pau, France

Received March 2, 2010. Revised manuscript received June 29, 2010. Accepted July 5, 2010.

Mercury (Hg) isotope composition was investigated in lichens over a territory of 900 km² in the northeast of France over a period of nine years (2001–2009). The studied area was divided into four geographical areas: a rural area, a suburban area, an urban area, and an industrial area. In addition, lichens were sampled directly at the bottom of chimneys, within the industrial area. While mercury concentrations in lichens did not correlate with the sampling area, mercury isotope compositions revealed both mass dependent and mass independent fractionation globally characteristic of each geographical area. Odd isotope deficits measured in lichens were smallest in samples close to industries, with $\Delta^{199}\text{Hg}$ of $-0.15 \pm 0.03\%$, where Hg is thought to originate mainly from direct anthropogenic inputs. Samples from the rural area displayed the largest anomalies with $\Delta^{199}\text{Hg}$ of $-0.50 \pm 0.03\%$. Samples from the two other areas had intermediate $\Delta^{199}\text{Hg}$ values. Mercury isotopic anomalies in lichens were interpreted to result from mixing between the atmospheric reservoir and direct anthropogenic sources. Furthermore, the combination of mass-dependent and mass independent fractionation was used to characterize the different geographical areas and discriminate the end-members (industrial, urban, and local/regional atmospheric pool) involved in the mixing of mercury sources.

Introduction

Mercury (Hg) is a hazardous pollutant discovered and used since the Roman period (1). From the beginning of the industrial era, anthropogenic fluxes to the atmosphere increased systematically and now dominate the natural fluxes, according to estimates from global modeling (1). It is believed that Hg deposition to eco- and geosystems has increased 3-fold compared to the estimated natural background over this time period (2). Regulations in different countries led many industrial companies to produce goods

with low Hg contents and to revise their removal systems and filters, but Hg emissions to the atmosphere from anthropogenic sources remain elevated (3, 4).

Gaseous elemental mercury (GEM) is the dominant species in the atmosphere. Because of its long atmospheric residence time, GEM is considered a transboundary pollutant because it may be deposited far from its emission source (5, 6). For this reason, atmospheric depositions at the scale of a small territory will represent mixtures between long-range transported GEM and gaseous oxidized mercury (GOM) from local sources with shorter lifetimes (5, 6). Deciphering the origin of pollution (global, regional, or local sources) or natural sources is crucial for developing policies for controlling mercury emission or deposition from human activities (2). However, tracing anthropogenic sources of heavy metals in a multiple source environment is currently a difficult task. Therefore, many such studies have been conducted around a single point source of pollution using multielement geochemistry (7, 8) or an isotopic approach. The latter mostly comprise Pb isotope tracing, but more recently other heavy metals such as Cd (9), Zn (10, 11), and Hg (12) were used as well. Identifying anthropogenic atmospheric sources using Pb isotopes measured in lichens, rain, and snow is possible because the compositions of potential sources are known (7, 13–16).

Mercury possesses several physicochemical features that may be used to understand and investigate pollution issues. Mercury concentration combined with its speciation are used to document the presence and the potential toxicity of a contamination. A third dimension of investigation has recently become available with the precise measurement of Hg isotope ratios, which shows that mass-dependent fractionation (MDF) of Hg isotopes could be used to trace anthropogenic emissions (12, 17–19) as well as natural sources (20–26). A fourth aspect has been recently added with the discovery of mass-independent fractionation (MIF) of Hg isotopes during photochemical or nonphotochemical reduction (22, 27, 28) as well as physical (29) and chemical (30) processes. Such MIF anomalies may be used to identify fractionation processes or sources in natural environments (18, 31–36). Combining these different analytical levels and scientific concepts would yield a deeper view of the complex issue of the origin and fate of Hg pollution in the environment.

This study reports the mercury isotopic composition of atmospheric matter recorded in lichens, sampled over a territory of 900 km² that contains multiple sources (anthropogenic and natural) and that was divided into four major geographical areas (rural, suburban, urban, and industrial). Sampling was performed over a period of nine years. The aim of the study is to show that MDF as well as MIF of Hg isotopes can discriminate multiple atmospheric sources and thus trace sources of environmental contamination.

Material and Methods

This study presents the Hg isotopic composition of lichens located in the northeast of France and covering an area of around 900 km² ($\approx 400\,000$ inhabitants). The main urban area is the city of Metz with 130 000 inhabitants (42 km²). Flatlands border this city to the south, east, and west, whereas an important industrial valley starts to the north of the city and continues to the Luxembourg border. Main wind directions are SW and NE (16). The territory was divided into four major geographical areas according mainly to the presence or absence of industrial/human activities (see Supporting Information (SI) Figure SI-S1). The four areas

* Corresponding author phone: +33 559407759; e-mail: nestrade@crpg.cnrs-nancy.fr.

† Nancy-Université.

‡ Université de Pau et des Pays de l'Adour.

are (1) Rural Area (RA, four sampling sites), (2) Suburban Area (SA, nine sampling sites), (3) Urban Area (UA, five sampling sites), (4) Industrial Valley (IV, five sampling sites). Within the IV, two lichens were sampled at two different industrial sites (I, two sampling sites). Eight species of epiphytic lichens were used for this study and sampled over a period of nine years (2001, 2003, 2006, 2008, and 2009). The Hg isotopic compositions of some of the lichens presented in this study were previously presented in Carignan et al. (33) (see SI Table SI-S1). Additional descriptions of all of these areas, types of lichens and sampling procedures are given in the SI.

Furthermore, particular attention was focused on a sampling site located within the suburban area (see SI Figure SI-S1). This point (CP-27) was identified as anomalous because of its high Hg concentration throughout the sampling years, with Hg contents three to four times higher than the average reported in all other geographical areas (see SI Table SI-S1 and results and discussion). Specific sampling of five lichens around this point was conducted in order to delimit this specific area. Additional descriptions concerning this contaminated point and the lichens sampled around it are given in the SI.

Lichens were freeze-dried according to the method described in Carignan and Gariepy (13) or dried at 105 °C and digested according to the method described in Estrade et al. 2010 (37). Hg concentrations were measured using either gas-chromatography coupled to ICP/MS or a solid Hg analyzer, as described in the SI. Isotopic analyses were performed using the MC-ICP-MS Nu Plasma HR (Nu Instruments) at the IPREM/LCABIE, Pau. Isotopic compositions are reported as recommended in Blum and Bergquist (38) relative to the NIST SRM 3133 Hg solution as defined for the $^{202}/^{198}\text{Hg}$ ratio:

$$\delta^{202/198}(\%)_{\text{sample}/\text{NIST3133}} = \left(\frac{^{202/198}\text{Hg}_{\text{sample}}}{^{202/198}\text{Hg}_{\text{NIST3133}}} - 1 \right) \times 1000$$

Mass independent fractionations measured on the odd ^{199}Hg and ^{201}Hg isotopes are expressed according to the definition of $\Delta^{199}\text{Hg}$ (%) and $\Delta^{201}\text{Hg}$ (%):

$$\Delta^{199}\text{Hg}(\%) = \delta^{199}\text{Hg}_{\text{measured}} - 0.252 \times \delta^{202}\text{Hg}_{\text{measured}}$$

$$\Delta^{201}\text{Hg}(\%) = \delta^{201}\text{Hg}_{\text{measured}} - 0.752 \times \delta^{202}\text{Hg}_{\text{measured}}$$

The external reproducibility of the method for this study was determined by 28 measurements of the secondary monoelemental reference material CRPG-RL24H. The two standard deviations measured were 0.19% on the $\delta^{202}\text{Hg}$, 0.05% and 0.07% on the $\Delta^{199}\text{Hg}$ (%) and $\Delta^{201}\text{Hg}$ (%), respectively. Analytical settings, analytical reproducibility of secondary monoelemental reference materials (CRPG-RL24H and UM-Almaden) as well as lichen BCR-482 reference material are reported in SI Table SI-S2 and discussed.

Results and Discussion

Long-Term Trends in Hg Concentrations in Lichens. Lichens in UA, SA, and RA were analyzed for their concentrations and are presented in SI Table SI-S1 and in SI Figure SI-S2 relative to the year and the lichen species. Relative standard deviations on the average concentration for individual points over the years of the study did not exceed 17% for a given lichen specie (UA-21, SA-07, SA-24, and RA-10, SA-12 excepted, see SI) and 24% when considering all lichen species sampled (UA-18, SA-14, SA-29, and RA-35). Moreover, no difference in concentration was measured between two different fruticose lichen species sampled the same year at a given site (RA-01). Furthermore, no significant trends

showing systematic increase or decrease in concentrations with time were observed (SI Table SI-S1 and Figure SI-S2). These results suggest that Hg concentrations did not show significant evolution through the years and that the different lichen species sampled may be considered as an homogeneous data set. For each geographical area, a representative Hg content was estimated by averaging the concentrations of all lichens retrieved since 2001. Hg concentrations in lichens in UA, SA, and RA displayed average values of, respectively, 108 ± 24 (SD, $n = 8$), 106 ± 17 (SD, $n = 15$), and 108 ± 34 (SD, $n = 9$) $\text{ng} \cdot \text{g}^{-1}$. Regarding lichens sampled only in 2009 within the industrial valley (IV), the average concentration was found to be 108 ± 24 $\text{ng} \cdot \text{g}^{-1}$ (SD, $n = 5$). No significant difference was found between these average Hg concentrations (one-way ANOVA, $F = 0.0264$, $p = 0.9941$, see SI). Lichens sampled at two industrial sites (I) presented an average concentration of 97 ± 26 (SD, $n = 2$), which is also in the range of all other areas. Thus, it appeared that Hg concentrations in lichens remained unchanged over a period of nine years and over a territory of 900 km^2 including various Hg emission sources (urban, industrial, natural).

Heavy metal uptake by lichens occurs by different processes such as wet, and particulate deposition but also results from gaseous adsorption. Accumulation in lichen implies very complex processes and is known to occur differently from one lichen to another (39, 40). In the case of mercury, the dominant specie (GEM) is homogeneously distributed in the global atmospheric reservoir, but next to the anthropogenic sources, lichens may preferentially sample oxidized and particulate Hg emitted by the chimneys. Horvat et al. (41) reported that the Hg content in lichens was a function of the contamination at the sampling site. However, Guevara et al. (42) reported that Hg concentrations in lichens from some background sites may be higher than samples located in contaminated sites (see also Garty et al. (39) for a compilation of Hg concentrations in lichens). Furthermore, Carignan et al. (33) reported high concentrations (around 2 $\mu\text{g} \cdot \text{g}^{-1}$) for lichens sampled in pristine areas of Canada (Hudson Bay) compared to samples retrieved from the Abitibi mining district further south. This may be explained by the high content of halogen elements in the atmosphere of the Hudson Bay area (43, 44) that would oxidize GEM and enhance the deposition rates and fluxes from the air to the lichens (45). Total gaseous mercury (TGM) concentrations measured in the Hudson Bay area are close to $2 \text{ ng} \cdot \text{m}^{-3}$ (46), very similar to our preliminary results for TGM measurements in the UA of Metz. The order of magnitude difference in lichen Hg content between the Hudson Bay area and Metz may be directly related to the abundance of oxidant elements present in the atmosphere. In contrast, lichens from the Abitibi mining area, 600–700 km inland south of Hudson Bay, yielded lichens having Hg contents only 2–3 times higher than those measured in Metz (45). The fact that Hg concentrations in lichens are very similar in space and time may indicate that there is no significant contrast in oxidant concentrations in the atmosphere of the Metz area.

Long-Term Trends in Isotopic Composition of Hg in Lichens. The Hg isotopic composition measured in lichens from all the sampling sites in function of the year and the species are presented in SI Table SI-S1. For all lichens, even isotopes (^{202}Hg , ^{200}Hg , ^{198}Hg) had relative abundances that follow a mass fractionation trend (MDF), whereas, odd mercury isotopes (^{201}Hg , ^{199}Hg) deviated from the MDF relationship suggesting MIF. The $\delta^{202}\text{Hg}$ values measured in all lichens ranged from -0.4 to -2.3 %. Recorded odd isotope anomalies were negative, in agreement with literature values reported for other lichens or mosses (32, 33) and ranged from -0.13 to -0.61 % for the $\Delta^{199}\text{Hg}$, with similar values for $\Delta^{201}\text{Hg}$. In addition to biophysico-chemical processes, which can fractionate Hg isotopes directly within the source (natural

TABLE 1. Average Concentrations and Isotopic Compositions (MDF and MIF) in Lichens for the Individual Geographical Areas

Sample Name	n ₁ ^a	n ₂ ^b	Hg range (ng.g ⁻¹)	Hg average (ng.g ⁻¹)	δ ²⁰² Hg	2SE	Δ ¹⁹⁹ Hg	2SE	Δ ²⁰¹ Hg	2SE	Δ ¹⁹⁹ Hg/Δ ²⁰¹ Hg	2SE
industrial sites	2	2	78–115	97	-1.90	0.19	-0.15	0.05	-0.16	0.07	0.94	0.16
industrial valley	4 ^d	5	82–148	108	-2.07	0.21	-0.27	0.05	-0.30	0.07	0.92	0.09
urban area	5	8	88–151	108	-0.95	0.29	-0.28	0.05	-0.38	0.07	0.73	0.03
suburb area	8 ^c	15	76–163	106	-1.00	0.19	-0.39	0.05	-0.46	0.07	0.86	0.04
rural area	4	9	77–177	108	-1.27	0.23	-0.50	0.05	-0.54	0.07	0.93	0.0

^a Number of sampling sites throughout the years in each geographical area. ^b Number of lichens used to calculate average concentrations and isotopic compositions. ^c SA-12 was removed from the calculations see SI. ^d IV-49 was removed from the calculations see SI.

or anthropogenic), transport as well as deposition processes of atmospheric Hg involving photochemistry, oxidation, and phase changes may also fractionate Hg isotopes. However, whereas the amplitude of fractionation is known for some reduction reactions, no data are available yet concerning the reactions that lead to Hg⁰ oxidation.

In this study, the sampling was a function of the geographical area, the time as well as the lichen specie. SI Figures SI-S3 and SI-S4 report, respectively, the δ²⁰²Hg and the Δ¹⁹⁹Hg for each sampling point as a function of the year and the lichen specie. Comparison of the δ²⁰²Hg and Δ¹⁹⁹Hg for the same lichen specie over the years indicates no significant changes for UA-21 and SA-24 and slight changes for SA-07 and RA-10. For a given year, comparison between different lichen species indicates no significant differences in δ²⁰²Hg for sites UA-18, RA-35, and RA-01 or in Δ¹⁹⁹Hg for sites UA-18, SA-14, SA-29, and RA-35. Slight differences in δ²⁰²Hg were observed between species for sites SA-14 and SA-29 and in Δ¹⁹⁹Hg only in site RA-01. Hence, similar to Hg concentrations, Hg isotopic compositions do not show any temporal trend and are not biased by the lichen specie analyzed. While further investigations remain necessary to better understand and constrain Hg uptake by lichens and associated isotopic fractionation, it appears that the Hg isotopic compositions of lichens at various sites are representative of the atmospheric Hg sampled by the lichen. Thus, isotopic compositions were averaged for all of the lichens collected at a given site throughout the years, as was done for concentrations. The average Hg isotope composition measured in lichens from the individual geographic areas is presented in Table 1. The δ²⁰²Hg was variable within a given geographical area, with a dispersion of ca. 1‰ for some zones. Differences between the average δ²⁰²Hg values of lichens in UA, SA, RA (-0.95 ‰, -1.00 ‰, -1.27 ‰, respectively) were found to be insignificant ($p \geq 0.1141$). Contrary to Hg concentrations, which did not differ between zones, the average δ²⁰²Hg value of lichens from the IV zone was significantly lighter (-2.07 ‰) than those measured for the three nonindustrial areas ($p \leq 0.0004$). Furthermore lichens sampled at the two industrial sites (I) within IV displayed similar δ²⁰²Hg (-1.90‰). This suggests that the Hg taken up by the lichens in the industrial area had different emission sources from that found in the urban, suburban, and rural areas. Furthermore, average Δ¹⁹⁹Hg measured in IV, UA, SA, and RA (see Table 1) were found to be significantly different from one area to another ($p \leq 0.0017$), also suggesting the contribution of different mercury sources.

Odd isotope deficits in lichens are believed to be representative of atmospheric Hg, which is the complementary reservoir of aquatic Hg in terms of isotope fractionation (33). This is because Hg(II) photoreduction of the aquatic reservoir yields positive Δ¹⁹⁹Hg and Δ²⁰¹Hg for residual Hg(II) with a Δ¹⁹⁹Hg/Δ²⁰¹Hg close to unity (22), whereas Hg in lichens have negative Δ¹⁹⁹Hg and Δ²⁰¹Hg, also with a Δ¹⁹⁹Hg/Δ²⁰¹Hg close to unity. The magnetic isotope effect (MIE) is responsible for these anomalies (22). Whereas lichens sampled in

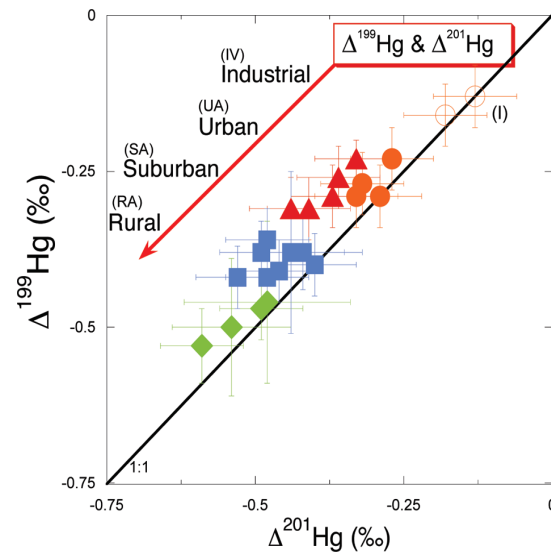


FIGURE 1. Average isotopic anomalies plotted as Δ¹⁹⁹Hg vs Δ²⁰¹Hg for the lichens sampled over the years 2001, 2003, 2006, 2008, and 2009 in the studied area. Rural Area (RA; ♦), Suburban Area (SA; ■), Urban Area (UA; ▲), Industrial Valley (IV; ●), Industrial sites (I; ○). In such an end-member model approach, a less negative odd isotope anomaly corresponds to a higher contribution of direct anthropogenic emissions.

I, IV, RA yielded Δ¹⁹⁹Hg/Δ²⁰¹Hg ratios falling on the 1:1 line (Figure 1), significant deviations were observed for all the lichens sampled in UA (average Δ¹⁹⁹Hg/Δ²⁰¹Hg = 0.74 ± 0.04 2SE, $n = 8$) and some lichens in SA. The ratio of anomalies suggests a higher ²⁰¹Hg deficit that is not in agreement with theoretical as well as experimental works which both suggest ratios between 1 and 1.3 for the MIE (22, 27, 47). Ratios between 1.6 and 2.45 are expected for the nuclear field shift effect (NFS) according to the nuclear charge radii used in the calculation (28–30, 32, 47).

Thus, all Δ¹⁹⁹Hg/Δ²⁰¹Hg ratios close to unity measured in lichens may readily be explained by MIE. However, Δ¹⁹⁹Hg/Δ²⁰¹Hg ratios lower than unity have rarely been reported in the literature (32). In the MIE theory, the amplitude of the odd isotope anomalies may be related to the absolute value of the magnetic moments of ¹⁹⁹Hg and ²⁰¹Hg (0.5029 and 0.5609 μ_B respectively). The resulting Δ¹⁹⁹Hg/Δ²⁰¹Hg ratio should be close to unity because of the similarity in the absolute magnetic moment values. However, the amplitude of anomalies may be controlled by other processes such as electron charge density and nuclear volume (48). The relative contributions of these processes according to the type of reaction may result in various Δ¹⁹⁹Hg/Δ²⁰¹Hg ratios (27, 28, 49), possibly lower than unity. Alternatively, mixing of Hg affected by MIE and NFS from two different reservoirs may yield apparently low ratios. Such processes have not yet been

identified in natural environments or demonstrated in experimental studies. Our findings indicate that more work is needed to understand MIF processes.

End Member Model Mixing Approach. Lichens from the RA displayed the largest anomaly with an average $\Delta^{199}\text{Hg}$ of $-0.50\text{‰} \pm 0.05$ (2SE, $n = 4$), followed by that of the SA with $-0.39\text{‰} \pm 0.05$ (2SE, $n = 8$). Lichens from both the UA and IV displayed average $\Delta^{199}\text{Hg}$ of $-0.28 \pm 0.05\text{‰}$ (2SE, $n = 5$) and $-0.27 \pm 0.05\text{‰}$ (2SE, $n = 5$), respectively. Finally, lichens sampled at industrial sites (I) within IV had $\Delta^{199}\text{Hg}$ of $-0.15 \pm 0.05\text{‰}$ (2SE, $n = 2$). The largest anomaly measured in lichens from remote areas yielded $\Delta^{199}\text{Hg}$ of ca. -1‰ , which was interpreted as the isotopic composition of the global atmospheric pool (33). Thus, any intermediate values between -1 and 0‰ may be viewed as mixtures between the global atmospheric pool (natural and/or anthropogenic Hg that cycled through photoreduction in both aquatic and terrestrial environments) and an end-member with no anomaly, possibly direct anthropogenic emissions. This is because most Hg or Hg-containing ore rocks and industrial materials display no Hg isotopic anomaly (19, 20, 23, 37). In this study, the fact that lichens sampled on industrial sites (I), had the smallest anomaly suggests that Hg originated mainly from nearby anthropogenic sources. This is also supported by very high Fe and other metal enrichment factors compared to other sites (≈ 4 -fold for Fe/Al and 3- and 7-fold for Cr/Al and Pb/Al respectively) shown by our preliminary unpublished data. Also, the measured $\Delta^{199}\text{Hg}$ value decreased with increasing distance from direct Hg anthropogenic sources to reach the most negative value in the rural area. These results reinforce the hypothesis formulated by Carignan et al. (33) concerning the end-members of the mixing model for the Hg isotopic composition in the atmosphere. Assessing the relative contributions from these two end-members may be possible assuming that the isotopic compositions of the Hg derived from the two mixing sources remained unchanged during transport and deposition. Currently, no data are available for photooxidation of GEM prior to its deposition, or oxidation in clouds, that may lead to MIF. Moreover, it is likely that lichen close to the stacks in the industrial valley did not sample the same Hg fraction as that sampled by lichens in other areas (probably more GOM and particulate Hg contribution in IV than other areas like SA and RA). Furthermore, whereas Carignan et al. (33) estimated that the global atmospheric Hg pool involved odd isotope deficits around -1‰ ($\Delta^{199}\text{Hg}$), Sherman et al. (36) investigated the isotopic composition of total gaseous mercury (TGM) in the arctic region and did not find significant negative isotope anomalies. However, these latter measurements represented the instantaneous isotopic composition of the atmosphere, whereas lichens sampled long-term deposition and adsorption of atmospheric Hg. Nevertheless, there is a possibility that the isotopic composition of the atmospheric pool varies with the geography. Currently, there are no data available on the isotopic composition of TGM in the city of Metz or in the surrounding areas. Because rural areas include a smaller proportion of direct anthropogenic sources, to a first approximation, an alternative end-member composition of -0.6‰ (the lower $\Delta^{199}\text{Hg}$ value in RA) can be suggested for the local/regional atmospheric pool. However, such a composition would imply that rural areas did not integrate Hg from direct anthropogenic inputs (such as those from UA or IV). Thus, considering that the atmospheric pool may vary at least between -0.6 and -1‰ , the contribution of direct anthropogenic sources to the total Hg measured in lichens would range from 50 to 75% in the lichens in UA.

Coupling MDF and MIF Anomalies in Lichens. Figure 2 presents $\Delta^{199}\text{Hg}$ plotted against $\delta^{202}\text{Hg}$ and composition fields for individual studied areas. Although lichens sampled within the IV area had slightly lower $\Delta^{199}\text{Hg}$ values, they displayed

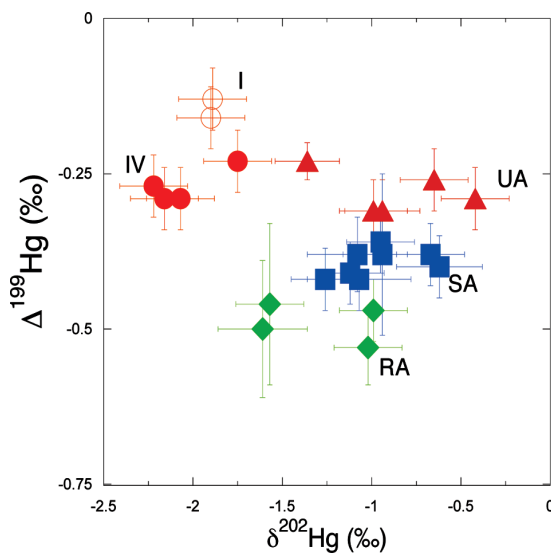


FIGURE 2. $\Delta^{199}\text{Hg}$ versus $\delta^{202}\text{Hg}$ for the lichens sampled over the years 2001, 2003, 2006, 2008, and 2009 in the studied area. Symbols as in Figure 1. MDF combined with MIF show significant differences in the signature found in IV and UA both affected by the same isotopic anomalies.

very similar $\delta^{202}\text{Hg}$ to those measured in lichens sampled on industrial sites (I), suggesting that Hg deposition within the valley mainly originates from the local industries. On the other hand, although having similar $\Delta^{199}\text{Hg}$, lichens from the UA have an average $\delta^{202}\text{Hg}$ values shifted toward heavier Hg, suggesting that Hg deposited from the atmosphere in the UA did not originate directly from the industrial valley. Thus, considering alteration of the isotopic composition during transport to be insignificant, direct anthropogenic input would have different sources in the IV and in the UA. Indeed, numerous potential anthropogenic sources may be present in the UA, such as domestic heating systems, small industrial complexes, commercial activities, road traffic, etc. As suggested by the similar $\delta^{202}\text{Hg}$ values, the direct anthropogenic contribution to atmospheric deposits in the SA and RA zones would also be of urban origin, and not "industrial" from the IV zone. This might be explained by the topography of the area and the main wind directions (SW and NE).

Figure 3 presents the average compositions of lichens in a $\Delta^{199}\text{Hg}$ versus $\delta^{202}\text{Hg}$ diagram. Lichen from the I and IV are individualized from the other zones suggesting again a different origin for Hg in the atmospheric deposits of these sites. The alignment of the data points in the two subgroups may be used to tentatively estimate the compositions of the source end-members. In such a scheme, anthropogenic Hg from the UA and the IV would have a similar $\Delta^{199}\text{Hg}$ close to zero but different $\delta^{202}\text{Hg}$ values of -0.40‰ and -1.75‰ respectively. Indeed, although lichens from the remote area close to Hudson Bay (Canada) have a $\Delta^{199}\text{Hg}$ close to -1‰ , $\delta^{202}\text{Hg}$ is closer to 0‰ . Adding these results to the diagram of Figure 3, a general negative relationship may be observed between $\Delta^{199}\text{Hg}$ and $\delta^{202}\text{Hg}$. Nevertheless, the scatter of the data points for the present study may suggest that more than two Hg sources are involved: the local/regional atmospheric pool, the industrial pool and an "urban" pool. Thus, whereas the Hg concentrations may be homogeneous throughout a large part of the atmospheric reservoir, the Hg isotopic composition (MDF and MIF) in the atmosphere is certainly representative of the site (contribution of natural versus anthropogenic sources). These end-members need to be verified but the combination of MDF and MIF is certainly

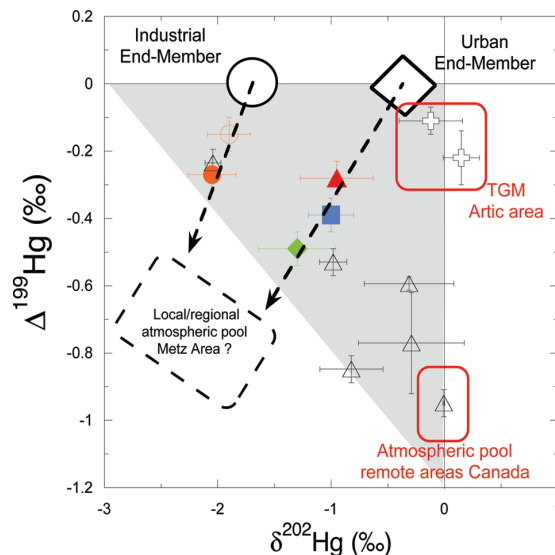


FIGURE 3. $\Delta^{199}\text{Hg}$ versus $\delta^{202}\text{Hg}$ for each individual geographical area. Symbols as in Figure 1. Relationship between RA, SA, and UA suggests mixing between urban Hg with $\delta^{202}\text{Hg}$; $\Delta^{199}\text{Hg}$ of -0.40% ; 0% and the local/regional atmospheric Hg pool having a lower $\Delta^{199}\text{Hg}$ value. End-member in IV is significantly different from that reported for the urban area with a $\delta^{202}\text{Hg}$; $\Delta^{199}\text{Hg}$ of -1.7% ; 0% . For comparison open triangles are lichens from the boreal forest of Québec (33) and open crosses are TGM in Barrow, Alaska (36). The distribution of the data points may be explained by a multisource system involving primarily Hg from industrial sources and the local/regional atmospheric pool.

useful for discriminating specific anthropogenic sources from the global atmospheric Hg pool.

Tracing a Mercury Point source. Lichen sample CP-27 (SI Figures SI-S1 and SI-S5 and Table SI-S1) displayed elevated Hg concentrations throughout the years (average [Hg] of ca. $400 \text{ ng} \cdot \text{g}^{-1}$). Furthermore, a distinct positive $\delta^{202}\text{Hg}$ averaging $+1.38\%$ (2SE , $n = 4$) was measured. These results contrast with all other Hg concentrations and isotopic compositions measured in the studied area and CP-27 was thus considered as a contaminated point. Samples from surrounding localities have Hg concentrations and isotopic compositions typical of the suburban area (SA/ACP 38–39–40–41). One sample (SA/ACP 42) located within 200 m of the contaminated point presented intermediate Hg concentration and isotopic composition ($[\text{Hg}] = 196 \text{ ng} \cdot \text{g}^{-1}$ and $\delta^{202}\text{Hg} = +0.46\%$, see SI Table SI-S1 and Figure SI-S6). Details on these particular sampling sites are given in the SI. The relationship between the contaminated point (CP-27), the intermediate point (SA/ACP 42) and the suburban average (mean of SA/ACP 38–39–40–41) is linear in the $\delta^{202}\text{Hg}$ vs $1/[\text{Hg}]$ diagram presented in Figure 4, strongly suggesting physical mixing between two mercury sources having distinct isotopic compositions and concentrations. The Hg-rich point source would have a high $\delta^{202}\text{Hg} \geq 1.5\%$ (Figure 4). A surprising observation is that these three points (one corresponds to the average suburban composition measured on five lichens) have negative $\Delta^{199}\text{Hg}$ anomalies of ca. -0.45% suggesting that MIF was already developed in the contaminant source/emission (SI Figure SI-S7). The exact nature of such a contamination is not known for now but our results strongly support the effectiveness of Hg isotopes for identifying various sources and types of emissions of atmospheric mercury.

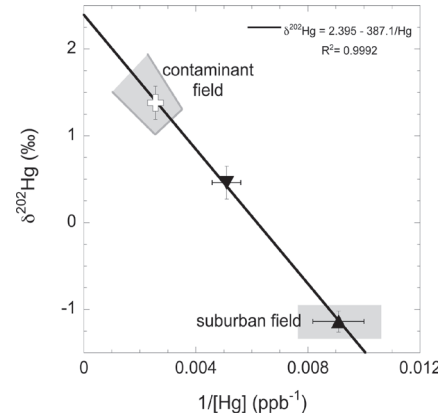


FIGURE 4. Data from the contaminated point (CP-27, open + sign), intermediate point (SA/ACP 42, ▼) and average suburban point (SA/ACP 38-39-40-41, ▲) in a $\delta^{202}\text{Hg}$ vs $1/[\text{Hg}]$ diagram suggesting physical mixing of two sources. The dispersion of the Hg-rich contaminant did not exceed 200 m.

Acknowledgments

We thank all the lichen samplers over the years (L. Marin, J. Banse, C. Cloquet, L. Fenet), Laurie Reisberg and Catherine Zimmermann (CRPG) for HPA assistance, Luc Marin and Jitka Lhomme (CRPG-SARM) for their technical support, S. Bouchet for GC-ICP/MS analyses, Remy Freydier and Sylvain Berail for analytical assistance on the LMTG Neptune and the IPREM Nu Plasma respectively. We also address special acknowledgments to Gaelle Deletraz for map realisation at the Laboratory "Société Environnement Territoire", University of Pau CNRS-UMR 5603 and Edwige Guerlet (IPREM/EEM) for her help with statistical calculations. We thank three anonymous reviewers for their constructive comments that greatly improved the manuscript. This work benefited from a CNRS EC2CO BIOMELI project grant. This is the CRPG contribution N° 2067.

Supporting Information Available

Additional data, tables, method descriptions and discussion. This material is available free of charge via the Internet at <http://pubs.acs.org>.

Literature Cited

- (1) Selin, N. E. Global Biogeochemical Cycling of Mercury: A Review. *Annu. Rev. Environ. Resour.* **2009**, *34*, 43–63.
- (2) Lindberg, S.; Bullock, R.; Ebinghaus, R.; Engstrom, D.; Feng, X. B.; Fitzgerald, W.; Pirrone, N.; Prestbo, E.; Seigneur, C. A synthesis of progress and uncertainties in attributing the sources of mercury in deposition. *Ambio* **2007**, *36* (1), 19–32.
- (3) Pacyna, E. G.; Pacyna, J. M.; Steenhuizen, F.; Wilson, S. Global anthropogenic mercury emission inventory for 2000. *Atmos. Environ.* **2006**, *40* (22), 4048–4063.
- (4) Pacyna, E. G.; Pacyna, J. M.; Fudala, J.; Strzelecka-Jastrzab, E.; Hlawiczka, S.; Panasiuk, D. Mercury emissions to the atmosphere from anthropogenic sources in Europe in 2000 and their scenarios until 2020. *Sci. Total Environ.* **2006**, *370* (1), 147–156.
- (5) Schroeder, W. H.; Munthe, J. Atmospheric mercury—An overview. *Atmos. Environ.* **1998**, *32* (5), 809–822.
- (6) Lin, C. J.; Pehkonen, S. O. The chemistry of atmospheric mercury: A review. *Atmos. Environ.* **1999**, *33* (13), 2067–2079.
- (7) Telmer, K.; Bonham-Carter, G. F.; Kliza, D. A.; Hall, G. E. M. The atmospheric transport and deposition of smelter emissions: Evidence from the multi-element geochemistry of snow, Quebec, Canada. *Geochim. Cosmochim. Acta* **2004**, *68* (14), 2961–2980.
- (8) Sterckeman, T.; Douay, F.; Proix, N.; Fourrier, H.; Perdrix, E. Assessment of the contamination of cultivated soils by eighteen trace elements around smelters in the North of France. *Water, Air, Soil Pollut.* **2002**, *135* (1–4), 173–194.

- (9) Cloquet, C.; Carignan, J.; Libourel, G.; Sterckeman, T.; Perdrix, E. Tracing source pollution in soils using cadmium and lead isotopes. *Environ. Sci. Technol.* **2006**, *40* (8), 2525–2530.
- (10) Sivry, Y.; Riote, J.; Sonke, J. E.; Audry, S.; Schafer, J.; Viers, J.; Blanc, G.; Freydier, R.; Dupre, B. Zn isotopes as tracers of anthropogenic pollution from Zn-ore smelters The Rio Mort-Lot River system. *Chem. Geol.* **2008**, *255* (3–4), 295–304.
- (11) Mattielli, N.; Petit, J. C. J.; Deboudt, K.; Flament, P.; Perdrix, E.; Taillez, A.; Rimetz-Plançon, J.; Weis, D. Zn isotope study of atmospheric emissions and dry depositions within a 5 km radius of a Pb-Zn refinery. *Atmos. Environ.* **2009**, *43* (6), 1265–1272.
- (12) Foucher, D.; Ogrinc, N.; Hintelmann, H. Tracing mercury contamination from the Idrija Mining Region (Slovenia) to the Gulf of Trieste using Hg isotope ratio measurements. *Environ. Sci. Technol.* **2009**, *43* (1), 33–39.
- (13) Carignan, J.; Gariepy, C. Isotopic composition of epiphytic lichens as a tracer of the sources of atmospheric lead emissions in southern Quebec, Canada. *Geochim. Cosmochim. Acta* **1995**, *59* (21), 4427–4433.
- (14) Simonetti, A.; Gariepy, C.; Carignan, J. Pb and Sr isotopic compositions of snowpack from Quebec, Canada: Inferences on the sources and deposition budgets of atmospheric heavy metals. *Geochim. Cosmochim. Acta* **2000**, *64* (1), 5–20.
- (15) Simonetti, A.; Gariepy, C.; Banic, C. M.; Tanabe, R.; Wong, H. K. Pb isotopic investigation of aircraft-sampled emissions from the Horne smelter (Rouyn, Quebec): Implications for atmospheric pollution in northeastern North America. *Geochim. Cosmochim. Acta* **2004**, *68* (16), 3285–3294.
- (16) Cloquet, C.; Carignan, J.; Libourel, G. Atmospheric pollutant dispersion around an urban area using trace metal concentrations and Pb isotopic compositions in epiphytic lichens. *Atmos. Environ.* **2006**, *40* (3), 574–587.
- (17) Biswas, A.; Blum, J. D.; Bergquist, B. A.; Keeler, G. J.; Xie, Z. Q. Natural mercury isotope variation in coal deposits and organic soils. *Environ. Sci. Technol.* **2008**, *42* (22), 8303–8309.
- (18) Laffont, L.; Sonke, J. E.; Maurice, L.; Hintelmann, H.; Pouilly, M.; Bacarreza, Y. S.; Perez, T.; Behra, P. Anomalous mercury isotopic compositions of fish and human hair in the Bolivian Amazon. *Environ. Sci. Technol.* **2009**, *43* (23), 8985–8990.
- (19) Stetson, S. J.; Gray, J. E.; Wanty, R. B.; Macalady, D. L. Isotopic variability of mercury in ore, mine-waste calcine, and leachates of mine-waste calcine from areas mined for mercury. *Environ. Sci. Technol.* **2009**, *43* (19), 7331–7336.
- (20) Smith, C. N.; Kesler, S. E.; Klaue, B.; Blum, J. D. Mercury isotope fractionation in fossil hydrothermal systems. *Geology* **2005**, *33* (10), 825–828.
- (21) Foucher, D.; Hintelmann, H. High-precision measurement of mercury isotope ratios in sediments using cold-vapor generation multi-collector inductively coupled plasma mass spectrometry. *Anal. Bioanal. Chem.* **2006**, *384* (7–8), 1470–1478.
- (22) Bergquist, B. A.; Blum, J. D. Mass-dependent and -independent fractionation of Hg isotopes by photoreduction in aquatic systems. *Science* **2007**, *318* (5849), 417–420.
- (23) Smith, C. N.; Kesler, S. E.; Blum, J. D.; Rytyuba, J. J. Isotope geochemistry of mercury in source rocks, mineral deposits and spring deposits of the California Coast Ranges, USA. *Earth Planet. Sci. Lett.* **2008**, *269* (3–4), 398–406.
- (24) Gehrke, G. E.; Blum, J. D.; Meyers, P. A. The geochemical behavior and isotopic composition of Hg in a mid-Pleistocene western Mediterranean sapropel. *Geochim. Cosmochim. Acta* **2009**, *73* (6), 1651–1665.
- (25) Sherman, L. S.; Blum, J. D.; Nordstrom, D. K.; McCleskey, R. B.; Barkay, T.; Vetriani, C. Mercury isotopic composition of hydrothermal systems in the Yellowstone Plateau volcanic field and Guaymas Basin sea-floor rift. *Earth Planet. Sci. Lett.* **2009**, *279* (1–2), 86–96.
- (26) Zambardi, T.; Sonke, J. E.; Toutain, J. P.; Sortino, F.; Shinohara, H. Mercury emissions and stable isotopic compositions at Vulcano Island (Italy). *Earth Planet. Sci. Lett.* **2009**, *277* (1–2), 236–243.
- (27) Zheng, W.; Hintelmann, H. Mercury isotope fractionation during photoreduction in natural water is controlled by its Hg/DOC ratio. *Geochim. Cosmochim. Acta* **2009**, *73* (22), 6704–6715.
- (28) Zheng, W.; Hintelmann, H. Nuclear field shift effect in isotope fractionation of mercury during abiotic reduction in the absence of light. *J. Phys. Chem. A* **2010**, *114* (12), 4238–4245.
- (29) Estrade, N.; Carignan, J.; Sonke, J. E.; Donard, O. F. X. Mercury isotope fractionation during liquid-vapor evaporation experiments. *Geochim. Cosmochim. Acta* **2009**, *73* (10), 2693–2711.
- (30) Wiederhold, J. G.; Cramer, C. J.; Daniel, K.; Infante, I.; Bourdon, B. K.; Kretzschmar, R. Equilibrium mercury isotope fractionation between dissolved Hg(II) species and thiol-bound Hg. *Environ. Sci. Technol.* **2010**, doi: 10.1021/es100205t.
- (31) Jackson, T. A.; Whittle, D. M.; Evans, M. S.; Muir, D. C. G. Evidence for mass-independent and mass-dependent fractionation of the stable isotopes of mercury by natural processes in aquatic ecosystems. *Appl. Geochem.* **2008**, *23* (3), 547–571.
- (32) Ghosh, S.; Xu, Y. F.; Huayun, M.; Odom, L. Mass-independent fractionation of mercury isotopes in the environment. *Geochem. Geophys. Geosyst.* **2008**, *9*.
- (33) Carignan, J.; Estrade, N.; Sonke, J. E.; Donard, O. F. X. Odd isotope deficits in atmospheric Hg measured in lichens. *Environ. Sci. Technol.* **2009**, *43* (15), 5660–5664.
- (34) Gantner, N.; Hintelmann, H.; Zheng, W.; Muir, D. C. Variations in stable isotope fractionation of Hg in food webs of arctic lakes. *Environ. Sci. Technol.* **2009**, *43* (24), 9148–9154.
- (35) Das, R.; Salters, V. J. M.; Odom, A. L. A case for in vivo mass-independent fractionation of mercury isotopes in fish. *Geochem. Geophys. Geosyst.* **2009**, *10*.
- (36) Sherman, L. S.; Blum, J. D.; Johnson, K. P.; Keeler, G. J.; Barres, J. A.; Douglas, T. A. Mass-independent fractionation of mercury isotopes in Arctic snow driven by sunlight. *Nat. Geosci.* **2010**, *3* (3), 173–177.
- (37) Estrade, N.; Carignan, J.; Sonke, J. E.; Donard, O. F. X. Measuring Hg isotopes in bio-geo-environmental reference materials. *Geostand. Geoanal. Res.* **2010**, *34* (1), 79–93.
- (38) Blum, J. D.; Bergquist, B. A. Reporting of variations in the natural isotopic composition of mercury. *Anal. Bioanal. Chem.* **2007**, *388* (2), 353–359.
- (39) Backor, M.; Loppi, S. Interactions of lichens with heavy metals. *Biol. Plant.* **2009**, *53* (2), 214–222.
- (40) Garty, J. Biomonitoring atmospheric heavy metals with lichens: Theory and application. CRC. *Crit. Rev. Plant Sci.* **2001**, *20* (4), 309–371.
- (41) Horvat, M.; Jeran, Z.; Spiric, Z.; Jacimovic, R.; Miklavcic, V. Mercury and other elements in lichens near the INA Naftaplin gas treatment plant, Molve, Croatia. *J. Environ. Monitor.* **2000**, *2* (2), 139–144.
- (42) Guevara, S. R.; Bubach, D.; Arribere, M. Mercury in lichens of Nahuel Huapi National Park, Patagonia, Argentina. *J. Radioanal. Nucl. Chem.* **2004**, *261* (3), 679–687.
- (43) Rose, E. F.; Carignan, J.; Chaussidon, M. Transfert of atmospheric Boron from oceans to continents: An investigation using precipitation waters and epiphytic lichens. *Geochem. Geophys. Geosyst.* **2000**, *1* (11), 1045.
- (44) Wen, H. J.; Carignan, J. Ocean to continent transfer of atmospheric Se as revealed by epiphytic lichens. *Environ. Pollut.* **2009**, *157* (10), 2790–2797.
- (45) Carignan, J.; Sonke, J. E., The effect of atmospheric mercury depletion events on the net deposition flux around Hudson Bay, Canada, *Atmos. Environ.* under revision.
- (46) Constant, P.; Poissant, L.; Villemur, R.; Yumvihoze, E.; Lean, D. Fate of inorganic mercury and methyl mercury within the snow cover in the low arctic tundra on the shore of Hudson Bay (Quebec, Canada). *J. Geophys. Res.-Atmos.* **2007**, *112* (D8).
- (47) Schauble, E. A. Role of nuclear volume in driving equilibrium stable isotope fractionation of mercury, thallium, and other very heavy elements. *Geochim. Cosmochim. Acta* **2007**, *71* (9), 2170–2189.
- (48) Krитеe, K.; Barkay, T.; Blum, J. D. Mass dependent stable isotope fractionation of mercury during mer mediated microbial degradation of monomethylmercury. *Geochim. Cosmochim. Acta* **2009**, *73* (5), 1285–1296.
- (49) Zheng, W.; Hintelmann, H. Isotope fractionation of mercury during its photochemical reduction by low-molecular-weight organic compounds. *J. Phys. Chem. A* **2010**, *114* (12), 4246–4253.

ES100674A

Supporting Information

Isotope Tracing of Atmospheric Mercury Sources in an Urban Area of Northeastern France

Nicolas Estrade, Jean Carignan and Olivier F.X. Donard

21 pages (including title page)

7 Figures (SI-S1 to SI-S7)

2 Tables (SI-S1 and SI-S2)

Lichens sampling description

In order to assure homogeneity of the sample and to perform multiple elemental and isotopic analyses, between 3 and 25 g of lichens hanging on tree branches were collected. The quantity sampled depended upon the lichen abundance at the sampling site. The sampling area at a given site depended also upon the lichen abundance and ranged from 100m² to around 1000m². Lichens were sampled between ground level and 2 meters high.

Living lichens were sampled mainly on thin tree branches (2 to 5 years old depending on the tree). Hence, we estimated that the age of the lichens sampled at a site may range from 2 to 5 years. The sampling of a large amount of material was aimed to recover homogeneous age fractions of lichens at each site.

When available, different species were separated at a given site. Indeed, because lichens do not have the same behaviour regarding atmospheric air composition, the same species were not present at each sampling site. Some lichens are airborne pollution sensitive (e.g. *Usnea* species) whereas others are pollution tolerant (e.g. *Xanthoria Parietina*). Thus, depending on the sampling site and the lichen diversity and abundance, 4 fruticose species (*Usnea* sp (US), *Ramalina farinacea* (RF), *Evernia prunastri* (EP), *Pseudevernia furfuracea* (PF)) and 4 foliose species were sampled (*Hypogymnia physodes* (HP), *Physcia tenella* (PT), *Xanthoria parietina* and/or *polycarpa* (XP)). Furthermore, several fruticose species could have been mixed (Mix F) to satisfy a sufficient amount of matter for homogeneity and analytical issues.

Lichens were sampled with gloves and plastic tweezers in order to avoid contact and inclusion of tree bark (specifically in the case of foliose species sampling). Then, samples were put into polyethylene bags prior to sample proceeding.

For most of the sites, sampling was done over the years 2001, 2003, 2006, 2008 and 2009. In total, the Hg isotopic composition of lichens was investigated at 31 sampling sites (Figure SI-S1) corresponding to 51 lichen samples analyzed. 10 of the 31 sampling sites

(corresponding to 19 of 51 lichen samples) were already presented in Carignan et al. (33). Information about type of lichen, sampling year and area, concentration and isotopic composition are given in Table SI-S1.

Sampling Sites Description

The region of study was divided into four major areas and one sub-area based (see Figure SI-S1) on quantitative criteria such as the inhabitant density, the presence or absence of industries, the proximity to anthropogenic emissions (road, commercial activities), the topography, the distance to the city of Metz, the density of forests and agricultural fields. Subdivisions identified were: rural area (RA), suburban area (SA), urban area (UA), industrial area (IV) and one sub-area located within the IV: industrial sites (I). In addition, one site with high Hg content measured in lichens drew our attention. Surroundings of this "contaminated point" (CP) located within the suburban area (Figure SI-S1) were sampled more intensively (SA/ACP). Descriptions of all these areas are given below.

Urban Area (UA, 5 sites). Sampling of the five lichen sites was done at the fringe of the historical centre, mainly because of the quantity of lichen available (distance from the city centre was less than 3 km). The population density within the urban area is 3000 inhab/km². Within this area, anthropogenic Hg sources may be multiple including domestic heating, urban traffic, one municipal waste incinerator, one coal and gas fired power plant.

Suburban Area (SA, 9 sites). This area is located between the rural area and the urban area (between 3 and 10 km from the city centre). With a density of inhabitants far less than in the urban area lichens were always sampled close to important roads or road connexions. Main anthropogenic Hg sources are a large coal fire power plant (500 MW) at the north of the city of Metz (in front of SA-12 sample, see Figure SI-S1), one waste combustor and domestic heating.

Rural Area (RA, 4 sites). This area comprised four sites sampled at a minimum of 12 Km from the city of Metz. Lichens were sampled at the edge of small woods surrounded by large cultivated fields and far from any roads, industrial activities or housing areas. Other than agricultural use (fertilizer, pesticides...), direct anthropogenic sources are scarce. Natural source emissions, such as soils or vegetation may be significant.

Industrial Valley (IV, 5 sites). The area covered in this study is the Southern part of the largest French industrial valley (Mosellan Valley), from Metz to Luxembourg. The studied area was located within the Orne Valley, which comprised an important number of iron mines and steel and iron factories. All the iron mines as well as many of the factories located within this valley were progressively closed during the 70-90's. Nevertheless, some large factories remain still active in the valley. Lichens IV-45 and IV-48 were sampled at the bottom of the valley (160 m elevation) whereas IV-46 and IV-47 were sampled at the top of the hills (250 and 350 m elevation respectively). IV-49 was sampled at a reconverted industrial site (now a large commercial mall).

Industrial sites (I, 2 sites). Two lichens were sampled at two different iron and steel factories still in operation at the time of the study, located within the industrial valley (IV). I-43 was sampled at the factory (steel industry and agglomerates) located in the town of Rombas (160 m elevation). Lichens were sampled just behind the fences of the factory on the west and south sides at around 50 to 100 meters of the stacks. I-44 was sampled at the factory (blast furnaces) located in the town of Gandrange (160 m elevation). Lichens were sampled just behind the fences of the factory on the south side from 50 to 200 meters of the stacks. For these two sites the foliose and fruticose lichen diversity was very low. Only two foliose lichen species were observed with a high abundance and identified as *xantoria parietina* and/or *xantoria polycarpa* (XP). *Xanthoria parietina* is known to be highly tolerant to airborne

pollution such as acid rain and heavy metals and thus are characteristic lichens found in the polluted area.

Contaminated point (CP-27, Figure SI-S5, 1 site) and Suburban Area Around the Contaminated Point (SA/ACP, Figure SI-S5, 5 sites). This point is located in the suburban area as shown on the general map (see Figure SI-S1). The contaminated point (CP-27) was found next to an agricultural field, a small wood, several houses and a highway, including a service area about 1 km away (Figure SI-S5). Lichens from this site have Hg concentrations ranging between 350 and 450 ng.g⁻¹ over the years 2001 to 2008 (see Table SI-S1). In order to trace the dispersion of Hg around this site, five lichens were sampled covering an area of 2 km² (see Figure SI-S5).

Analytical Methods

All the lichens (other the ones reported in Carignan et al. (33)) were dried in the laboratory (105°C during at least 24 hours) or freeze-dried according to the method reported by Carignan and Gariépy (13). Between 0.5 and 1.5 g of dried matter was introduced into 6 ml of concentrated HNO₃ prior to achieve the high temperature and high pressure digestion method applied to the lichen reference material BCR-482 described in Estrade et al. (37).

Hg concentrations of lichens sampled from 2001 to 2008 were analysed after digestion using Gas chromatography-isotope-dilution coupled to Thermo-Finnigan X2 ICP-MS (Institut Pluridisciplinaire de Recherche sur l'Environnement et les Matériaux (IPREM) in Pau) according to the method described in Montperrus et al. In order to assure 100% digestion yield, multiple digestions of the lichen reference material BCR-482 were performed as well as digestion of lichens already analysed in Carignan et al. (33) (e.g. RA-10, RA-35) and duplicate of digestion (RA-01) (see Table S1). Hg concentrations of lichens sampled in 2009 were determined on dry material by using the mercury analyser Milestone DMA-80®. Here,

multiple digestions of the BCR-482 were also done as well as digestion duplicate (e.g. IV-47).

Digestion yields were directly measured comparing the intensity of the sample relative to the reference material NIST 3133 in the same acidic matrix on the MC-ICP-MS before the isotopic analysis.

The isotopic compositions of lichens were analyzed by using a cold-vapor generation system (home-made gas-liquid separator, see Estrade et al. (37)) coupled to a Nu Plasma HR (Nu Instruments, UK) MC-ICP-MS at the IPREM/LCABIE in Pau, as described in Estrade et al. (37). Digested lichens as well as the NIST SRM 3133 reference material "delta zero" were diluted in a similar acidic matrix (between 10 and 20% HNO₃ v/v) to appropriate Hg concentrations (3 to 5 µg.L⁻¹) and Hg(II) was reduced on line with 3% w/v SnCl₂ (Alfa Aesar NormaPur) in 1 mol.L⁻¹ supra pur HCl. The instrumental mass bias drift was monitored by using the standard-sample-standard bracketing method and NIST SRM 997 Thallium as the internal reference and corrected with the exponential mass fractionation law. The Thallium was continuously introduced using a desolvation unit (DSN). Mixing with Hg⁰ was done into the ICP-MS torch using a double input torch. Additional descriptions are provided in Estrade et al. (37).

Variations in Hg isotopic composition are expressed relative to the standard reference material NIST SRM 3133, using the delta notation and following recent recommendations for Hg isotope measurement (Blum and Bergquist (38)):

$$\delta^{X/198}(\text{‰})_{\text{sample/NIST3133}} = \left(\frac{\text{Hg}_{\text{sample}}}{\text{Hg}_{\text{NIST3133}}} - 1 \right) \times 1000.$$

where X represents Hg isotopes other than 198. Mass Independent Fractionation (MIF) are expressed as described in Blum and Bergquist (38)

$$\Delta^{199}\text{Hg} = \delta^{199}\text{Hg}_{\text{measured}} - 0.252 \times \delta^{202}\text{Hg}_{\text{measured}}$$

$$\Delta^{200}\text{Hg} = \delta^{200}\text{Hg}_{\text{measured}} - 0.502 \times \delta^{202}\text{Hg}_{\text{measured}}$$

$$\Delta^{201}\text{Hg} = \delta^{201}\text{Hg}_{\text{measured}} - 0.752 \times \delta^{202}\text{Hg}_{\text{measured}}$$

$$\Delta^{204}\text{Hg} = \delta^{204}\text{Hg}_{\text{measured}} - 1.493 \times \delta^{202}\text{Hg}_{\text{measured}}$$

For this study the long term external reproducibility of the method was determined by repeated analyses of the secondary mono-elemental reference material CRPG-RL24H for which our results were compared to published values in Estrade et al. (37). The external reproducibility of unknown samples was calculated as 2 standard errors (2SE) of the mean value (from different brackets of the sample), except when this value was lower than the external reproducibility of the method. The isotopic composition of multiple digestions ($n=5$) of the lichen reference material BCR-482 was in agreement with the value determined in Estrade et al. (37). Added to these reference materials, we started to run during the last analysis session the well-characterized UM-Almaden material that showed also results in agreement with the published values (Blum and Bergquist (38)). All the results are reported in Table SI-S2.

Statistical calculations

All statistical analyses were undertaken with STATISTICA software, version 5.5 (StatSoft, USA). The mercury concentrations, $\delta^{202}\text{Hg}$, $\Delta^{199}\text{Hg}$ and $\Delta^{201}\text{Hg}$ were tested by one-way analysis of variance (ANOVA) in order to investigate the effects of sampling areas on the concentration and isotopic results in lichens (degree of freedom =3). Significant differences between paired means were determined by Tukey HSD for unequal N (Spjotvol Stoline). Prior to analysis, homoscedasticity was assessed by Brown-Forsythe test. For all statistical analysis, the significance level was set at $\alpha = 0.05$. The dataset tested included geographical areas UA, SA, RA and IV. Area I was not taken into account because only two samples were available to perform statistical tests.

Additional comments on data points removed from calculations

In order to define average isotopic compositions for each individual area, SA-12 was removed from calculations because of its non-homogeneity between 2003 and 2008. Indeed, its concentration decreased two fold and the $\Delta^{199}\text{Hg}$ values changed also drastically between these two years. This change in concentration and isotopic composition indicated either a bias in the sampling (e.g. sampling of dead or young lichens) or variation in Hg atmospheric fallout for this given site. In addition, the point IV-49 was removed from calculations because $\Delta^{199}\text{Hg}$ measured ($-0.39 \pm 0.05\text{\textperthousand}$) at this point contrasted with the average defined by other sampling sites in the industrial valley ($-0.27\text{\textperthousand}$). In fact, point IV-49 was sampled above a slag heap, while all other sites represent converted industrial sites into commercial and recreational areas since 15 years. Point IV-49 was thus considered as more representative of the suburban area than of the industrial valley.

Additional comments on the Contaminated point (CP-27) and Suburban Area Around the Contaminated Point (SA/ACP). This study is located in the suburban area as showed on Figure SI-S1. The contaminated point was found throughout the years to display an average [Hg] of 400 ng.g^{-1} and a $\delta^{202}\text{Hg}$, averaging at $+1.38 \pm 0.19\text{\textperthousand}$ associated with a $\Delta^{199}\text{Hg}$ of $-0.49 \pm 0.12\text{\textperthousand}$ (CP-27, 2SE n=4, Tab. SI-S1). The lichen SA/ACP-42 was sampled in front of CP-27 on the other side of the highway at c.a. 200 meters away and presents Hg concentration of 196 ng.g^{-1} also, high regarding all others lichens of this area (see Table SI-S1 and Figure SI-S6). Furthermore, this lichen displays a $\delta^{202}\text{Hg} +0.46 \pm 0.19\text{\textperthousand}$ that is lighter than CP-27, but heavier than all other lichens from suburban area. It shows a similar $\Delta^{199}\text{Hg}$ ($-0.42 \pm 0.05\text{\textperthousand}$) to SA/ACP lichens (see Fig SI-S7). Lichens SA/ACP 38-39-40-41 were sampled over 200m away from CP-27 and show Hg concentrations in the average determined for all others lichens of the study ($80-130 \text{ ng.g}^{-1}$, Table SI-S1 and Figure SI-S6) with isotopic compositions

in the range determined for the suburban area ($\delta^{202}\text{Hg} = -1.14 \pm 0.12\text{\textperthousand}$; $\Delta^{199}\text{Hg} = -0.42 \pm 0.05\text{\textperthousand}$ and $\Delta^{201}\text{Hg} = -0.46 \pm 0.06\text{\textperthousand}$, 2SE, n=4). Figure SI-S7 presents the $\Delta^{199}\text{Hg}$ versus the $\delta^{202}\text{Hg}$ of the contaminated point (CP-27) and lichens sampled in the surrounding area. It clearly shows that this contamination source has a small-scale impact, probably limited to a few hundred meters.

Literature cited

Monperrus, M.; Tessier, E.; Veschambre, S.; Amouroux, D.; Donard, O.,
Simultaneous speciation of mercury and butyltin compounds in natural waters and snow by
propylation and species-specific isotope dilution mass spectrometry analysis. *Anal. Bioanal. Chem.* **2005**, 381, (4), 854-862.

TABLES

TABLE SI-S1: Summary of sampling year, type of lichens, Hg concentrations and mercury isotope compositions of lichens sampled on the different geographical areas of the study

Sample Name	Year	Lichen species (ng g ⁻¹)	n ^{b)}	RSD (%) ^{a)}	Study ^{c)}	$\delta^{199}\text{Hg}$	2SE	$\delta^{200}\text{Hg}$	2SE	$\delta^{202}\text{Hg}$	2SE	$\delta^{204}\text{Hg}$	2SE	$\Delta^{199}\text{Hg}$	2SE	$\Delta^{200}\text{Hg}$	2SE	$\Delta^{202}\text{Hg}$	2SE	$\Delta^{199}\text{Hg}/\Delta^{201}\text{Hg}$				
Urban Area (UA)																								
UA-21A	2001	HP	88	1	A	-0.57	-0.64	-1.37	-1.42	-0.22	0.07	-0.30	0.71											
UA-21	2006	HP	91	1	A	-0.57	-0.52	-1.33	-1.30	-0.24	0.13	-0.35	0.68											
UA-21			90	2		-0.57	0.01	-0.58	0.18	-1.35	0.07	-1.36	0.18	-0.23	0.03	0.10	0.09	-0.33	0.07	0.69				
UA-17	2008	EP	134	13	B	-0.56	0.07	-0.49	0.09	-1.15	0.13	-0.99	0.19	-1.55	0.29	-0.31	0.05	0.01	0.06	-0.41	0.07	-0.08	0.15	
UA-18	2003	HP	97	1	A	-0.62	-0.50	-1.33	-1.11	-0.34	0.06	-0.49	0.69											
UA-18a	2006	EP	93	1	A	-0.51	-0.36	-0.98	-0.75	-0.32	0.02	-0.41	0.77											
UA-18	2008	Us+EP	86	1	B	-0.52	0.07	-0.44	0.09	-1.14	0.13	-0.97	0.19	-1.33	0.29	-0.28	0.05	0.06	-0.41	0.07	0.11	0.15		
UA-18			92	6		-0.55	0.07	-0.43	0.09	-1.15	0.20	-0.94	0.21	-1.33	0.29	-0.31	0.05	0.04	0.06	-0.44	0.07	0.11	0.15	
UA-16	2008	EP	151	15	B	-0.43	0.07	-0.28	0.09	-0.85	0.13	-0.65	0.19	-1.04	0.29	-0.26	0.05	0.04	0.06	-0.36	0.07	-0.07	0.15	
UA-15	2008	EP	125	13	1	B	-0.40	0.07	-0.16	0.09	-0.69	0.13	-0.42	0.19	-0.72	0.29	-0.29	0.05	0.06	-0.37	0.07	-0.09	0.15	
Suburb Area (SA)																								
SA-07	2003	EP	110	1	A	-0.71	-0.51	-1.32	-1.10	-0.43	0.04	-0.49	0.88											
SA-07	2006	EP	93	1	A	-0.67	-0.39	-1.19	-0.92	-0.44	0.07	-0.50	0.88											
SA-07	2008	EP	78	2	B	-0.48	0.12	-0.32	0.13	-0.94	0.20	-0.79	0.27	-1.33	0.29	-0.28	0.05	0.07	0.06	-0.35	0.07	-0.15	0.15	
SA-07			94	17		-0.62	0.17	-0.41	0.13	-1.15	0.27	-0.94	0.22	-1.33	0.29	-0.38	0.13	0.06	0.06	-0.44	0.12	-0.15	0.15	
SA-12B	2003	HP	163	1	A	-0.77	-0.73	-1.71	-1.61	-0.36	0.08	-0.50	0.73											
SA-12	2008	HP	83	1	B	-0.61	0.07	-0.73	0.09	-1.45	0.13	-1.58	0.19	-2.42	0.29	-0.21	0.05	0.06	-0.27	0.07	-0.06	0.15		
SA-12			123	46		-0.69	0.07	-0.73	0.09	-1.58	0.13	-1.59	0.19	-2.42	0.29	-0.29	0.15	0.07	0.06	-0.38	0.23	-0.06	0.15	
SA-13	2008	EP	91	9	1	B	-0.55	0.07	-0.30	0.09	-0.99	0.13	-0.67	0.19	-0.94	0.29	-0.38	0.05	0.04	0.06	-0.49	0.07	0.07	0.15

Sample Name	Year	Lichen species	Hg ¹ , (ng g ⁻¹)	RSD (%) ^{a)}	n ^{b)}	Study ^{c)}	$\delta^{199}\text{Hg}$	2SE	$\delta^{200}\text{Hg}$	2SE	$\delta^{202}\text{Hg}$	2SE	$\delta^{204}\text{Hg}$	2SE	$\Delta^{198}\text{Hg}$	2SE	$\Delta^{200}\text{Hg}$	2SE	$\Delta^{201}\text{Hg}$	2SE	$\Delta^{199}\text{Hg}/\Delta^{201}\text{Hg}$			
SA-14a	2001	HP	105	1	A	-0.71	-0.56	-1.43	-1.21	-0.41	0.04	-0.52	0.79	-0.52	0.04	-0.46	0.04	-0.46	0.04	0.93				
SA-14a	2003	HP	111	1	A	-0.74	-0.58	-1.38	-1.23	-0.43	0.04	-0.46	0.79	-0.52	0.04	-0.46	0.04	-0.46	0.04	0.93				
SA-14	2008	EP, PF	136	1	B	-0.61	0.07	-0.39	0.09	-1.07	0.13	-0.79	0.19	-1.38	0.29	-0.41	0.05	0.01	0.06	-0.47	0.07	-0.21	0.15	
SA-14	2008	EP, PF	117	14		-0.69	0.08	-0.51	0.12	-1.29	0.23	-1.07	0.29	-1.38	0.29	-0.42	0.05	0.03	0.06	-0.48	0.07	-0.21	0.15	
SA-23	2008	EP	101	10	2	B	-0.55	0.08	-0.28	0.12	-0.87	0.22	-0.62	0.24	-0.96	0.30	-0.40	0.05	0.03	0.06	-0.40	0.07	-0.04	0.15
SA-29	2001	RF	118	1	A	-0.62	-0.36	-1.11	-0.87	-0.40	0.08	-0.46	0.87	-0.46	-0.40	0.08	-0.46	0.08	-0.46	0.08	0.87			
SA-29	2003	HP	118	1	A	-0.68	-0.62	-1.40	-1.35	-0.34	0.05	-0.39	0.88	-0.39	-0.34	0.05	-0.39	0.05	-0.39	0.05	0.88			
SA-29a	2006	EP	130	1	A	-0.65	-0.47	-1.19	-1.01	-0.39	0.04	-0.42	0.92	-0.42	-0.39	0.04	-0.42	0.04	-0.42	0.04	0.92			
SA-29	2006	EP	122	6		-0.65	0.04	-0.48	0.15	-1.23	0.17	-1.08	0.28	-0.38	0.06	0.06	0.04	-0.42	0.07	0.00	0.15			
SA-37	2008	Mix F	121	12	1	B	-0.60	0.07	-0.46	0.09	-1.20	0.13	-0.95	0.19	-1.51	0.29	-0.36	0.05	0.02	0.06	-0.48	0.07	-0.08	0.15
SA-24	2006	EP	76	1	A	-0.68	-0.52	-1.34	-1.09	-0.41	0.03	-0.51	0.75	-0.51	-0.41	0.05	-0.51	0.03	-0.51	0.03	0.75			
SA-24	2008	EP	90	1	B	-0.69	0.07	-0.58	0.09	-1.27	0.13	-1.14	0.19	-1.71	0.29	-0.41	0.05	-0.01	0.06	-0.41	0.07	0.00	0.15	
SA-24	2008	EP	83	12		-0.69	0.07	-0.55	0.09	-1.30	0.13	-1.12	0.19	-1.71	0.29	-0.41	0.05	0.01	0.06	-0.46	0.07	0.00	0.15	
SA-19	2008	Mix F	108	11	1	B	-0.74	0.07	-0.60	0.09	-1.48	0.13	-1.26	0.19	-1.94	0.29	-0.42	0.05	0.04	0.06	-0.53	0.07	-0.06	0.15
Rural Area (RA)																								
RA-10A	2003	EP, PF	85	1	A	-0.99	-0.88	-1.89	-1.74	-0.55	0.00	-0.59	0.94	-0.59	-0.55	0.00	0.06	-0.49	0.07	0.11	0.15			
RA-10	2003	EP, PF	88	1	B	-0.82	0.07	-0.69	0.09	-1.61	0.13	-1.49	0.19	-2.11	0.29	-0.44	0.05	0.06	0.06	-0.49	0.07	0.11	0.15	
RA-10	2003	EP, PF	87	2		-0.90	0.17	-0.78	0.19	-1.75	0.28	-1.61	0.25	-2.11	0.29	-0.50	0.11	0.03	0.07	-0.54	0.10	0.11	0.15	
RA-35	2001	EP, PF	140	2	B	-0.69	0.16	-0.40	0.17	-1.22	0.19	-0.89	0.22	-1.33	0.46	-0.46	0.10	0.04	0.06	-0.55	0.03	0.00	0.13	
RA-35	2003	EP, PF	130	1	A	-0.84	-0.41	-1.33	-0.90	-0.61	0.04	-0.61	0.04	-0.61	0.29	-0.55	0.05	0.07	0.06	-0.65	0.04	0.00	0.85	
RA-35	2003	EP, PF	177	1	B	-0.82	0.07	-0.47	0.09	-1.40	0.13	-1.07	0.19	-1.68	0.29	-0.55	0.05	0.07	0.06	-0.60	0.07	-0.08	0.15	
RA-35B	2006	US	97	1	A	-0.82	-0.61	-1.47	-1.21	-0.51	0.00	-0.56	0.00	-0.56	0.00	-0.56	0.00	-0.56	0.00	-0.56	0.00	0.91		
RA-35	2006	US	136	24		-0.79	0.07	-0.47	0.09	-1.35	0.13	-1.02	0.19	-1.50	0.29	-0.53	0.06	0.04	0.06	-0.59	0.07	-0.04	0.15	

Sample Name	Year	Lichen specie	Hg (ng g ⁻¹)	RSD (%) ^{a)}	n ^{b)}	Study ^{c)}	$\delta^{199}\text{Hg}$	2SE	$\delta^{200}\text{Hg}$	2SE	$\delta^{201}\text{Hg}$	2SE	$\delta^{202}\text{Hg}$	2SE	$\delta^{203}\text{Hg}$	2SE	$\Delta^{199}\text{Hg}$	2SE	$\Delta^{200}\text{Hg}$	2SE	$\Delta^{201}\text{Hg}$	2SE	$\Delta^{202}\text{Hg}$	2SE	$\Delta^{199}\text{Hg}/\Delta^{201}\text{Hg}$
RA-03	2008	Mix F	98	10	2	B	-0.72	0.07	-0.43	0.09	-1.23	0.13	-0.99	0.19	-1.49	0.29	-0.47	0.05	0.06	-0.49	0.07	-0.02	0.15	0.96	
RA-01	2008	EP	77	1	B	-0.77	0.07	-0.70	0.09	-1.53	0.13	-1.49	0.19	-2.17	0.29	-0.40	0.05	0.05	0.06	-0.41	0.07	0.05	0.15	0.97	
RA-01	2008	RF	78	2	B	-0.94	0.07	-0.82	0.09	-1.78	0.13	-1.64	0.19	-2.41	0.29	-0.53	0.05	0.00	0.06	-0.55	0.07	0.04	0.15	0.97	
RA-01			77	1		-0.86	0.07	-0.76	0.09	-1.66	0.13	-1.57	0.19	-2.29	0.29	-0.46	0.13	0.02	0.07	-0.48	0.14	0.05	0.02	0.97	
Industrial Sites (I)																									
I-43	2009	XP	78	8	1	B	-0.64	0.07	-0.93	0.09	-1.61	0.13	-1.90	0.19	-2.91	0.29	-0.16	0.05	0.02	0.06	-0.18	0.07	-0.07	0.15	0.90
I-44	2009	XP	115	12	2	B	-0.60	0.07	-0.90	0.09	-1.55	0.13	-1.89	0.19	-2.94	0.29	-0.13	0.05	0.04	0.06	-0.13	0.07	-0.13	0.15	0.96
Industrial Valley (IV)																									
IV-45	2009	HP, PT	82	8	2	B	-0.67	0.07	-0.83	0.09	-1.59	0.13	-1.75	0.19	-2.72	0.29	-0.23	0.05	0.05	0.06	-0.27	0.07	-0.11	0.15	0.84
IV-46	2009	HP, PT	148	15	1	B	-0.83	0.07	-1.11	0.09	-1.99	0.13	-2.22	0.19	-3.34	0.29	-0.27	0.05	0.01	0.06	-0.32	0.07	-0.03	0.15	0.83
IV-47	2009	HP, PT	107	2	B	-0.85	0.07	-1.06	0.09	-1.93	0.13	-2.19	0.19	-3.31	0.29	-0.30	0.05	0.04	0.06	-0.28	0.07	-0.04	0.15	1.06	
IV-47	2009	HP, PT	107	1	B	-0.81	0.07	-1.04	0.09	-1.90	0.13	-2.13	0.19	-3.26	0.29	-0.28	0.05	0.03	0.06	-0.30	0.07	-0.08	0.15	0.93	
IV-47			107	11		-0.83	0.07	-1.05	0.09	-1.91	0.13	-2.16	0.19	-3.28	0.29	-0.29	0.05	0.04	0.06	-0.29	0.07	-0.06	0.15	0.99	
IV-48	2009	HP, PT	98	10	2	B	-0.81	0.07	-1.02	0.09	-1.89	0.13	-2.07	0.19	-3.16	0.29	-0.29	0.05	0.03	0.06	-0.33	0.07	-0.06	0.15	0.87
IV-49	2009	HP, PT	120	12	2	B	-0.88	0.04	-0.94	0.08	-1.87	0.08	-1.94	0.25	-2.89	0.37	-0.39	0.05	0.04	0.06	-0.41	0.11	0.01	0.00	0.96
Contaminated point (CP)																									
CP-27	2001	EP	338	2	A	-0.32	0.63	0.30	1.24								-0.64	0.00							1.01
CP-27	2003	Mix F	350	2	A	-0.05	0.69	0.66	1.40								-0.40	-0.01							0.99
CP-27	2006	EP	450	2	A	-0.16	0.72	0.58	1.50								-0.54	-0.03							0.99
CP-27	2008	HP	424	2	B	-0.03	0.07	0.69	0.09	0.69	0.13	1.37	0.19	2.00	0.29	-0.38	0.05	0.00	0.06	-0.34	0.07	-0.04	0.15	1.12	
CP-27			391	14		-0.14	0.13	0.68	0.09	0.56	0.17	1.38	0.19	2.00	0.29	-0.49	0.12	-0.01	0.06	-0.48	0.13	-0.04	0.15	1.03	

Sample Name	Year	Lichen species (ng g ⁻¹)	Hg ^{n^b} (%) ^{a)}	RSR	$\delta^{199}\text{Hg}$	2SE	$\delta^{200}\text{Hg}$	2SE	$\delta^{202}\text{Hg}$	2SE	$\delta^{204}\text{Hg}$	2SE	$\Delta^{199}\text{Hg}$	2SE	$\Delta^{200}\text{Hg}$	2SE	$\Delta^{202}\text{Hg}$	2SE	$\Delta^{204}\text{Hg}$	2SE	$\Delta^{199}\text{Hg}/\Delta^{201}\text{Hg}$				
Suburb Area Around Contaminated Point (SA/ACP)																									
SA/ACP-38	2009	RF,EP	88	9	1	B	-0.67	0.07	-0.43	0.09	-1.21	0.13	-0.99	0.19	-1.55	0.29	-0.42	0.05	0.07	0.06	-0.46	0.07	-0.06	0.15	0.90
SA/ACP-39	2009	RF,EP	81	8	2	B	-0.66	0.07	-0.54	0.09	-1.29	0.13	-1.21	0.19	-1.98	0.29	-0.36	0.05	0.06	-0.38	0.07	-0.18	0.15	0.94	
SA/ACP-40	2009	RF,EP	133	13	1	B	-0.77	0.07	-0.49	0.09	-1.32	0.13	-1.11	0.19	-1.88	0.29	-0.49	0.05	0.07	0.06	-0.49	0.07	-0.23	0.15	0.99
SA/ACP-41	2009	RF,EP	92	9	1	B	-0.73	0.07	-0.56	0.09	-1.46	0.13	-1.25	0.19	-1.88	0.29	-0.42	0.05	0.07	0.06	-0.52	0.07	-0.01	0.15	0.79
SA/ACP-42	2008	RF,EP	196	20	1	B	-0.30	0.07	0.24	0.09	-0.10	0.13	0.46	0.19	0.54	0.29	-0.42	0.05	0.01	0.06	-0.44	0.07	-0.15	0.15	0.94

a) Relative standard deviation indicated except if only one sample was analyzed. In this case, a SD of 10% was reported
 b) number of measurements
 c) A: Carnahan et al. 2009; B: This study

TABLE SI-S2: Isotopic compositions of reference material CRPG RRL24H, BCR-482 and UM-Almaden																			
Sample	n ^{a)}	$\delta^{199}\text{Hg}$	2SD	$\delta^{200}\text{Hg}$	2SD	$\delta^{201}\text{Hg}$	2SD	$\delta^{204}\text{Hg}$	2SD	$\Delta^{199}\text{Hg}$	2SD	$\Delta^{200}\text{Hg}$	2SD	$\Delta^{201}\text{Hg}$	2SD	$\Delta^{204}\text{Hg}$	2SD		
CRPG-RL24H	28	0.60	0.07	1.29	0.09	1.89	0.13	2.58	0.19	3.87	0.29	-0.05	0.05	-0.01	0.06	-0.05	0.07	0.02	0.15
BCR-482	10	-0.98	0.09	-0.75	0.11	-1.86	0.16	-1.68	0.26	-2.62	0.32	-0.56	0.07	0.09	0.06	-0.60	0.05	-0.11	0.10
UM-Almaden	5	-0.18	0.03	-0.32	0.01	-0.48	0.07	-0.61	0.14	-0.94	0.23	-0.03	0.02	-0.02	0.06	-0.02	0.03	-0.03	0.10

a) number of measurements

FIGURES

FIGURE SI-S1: General map of the sampling locations and sampling points in Rural Area (RA), Suburban Area (SA), Urban Area (UA), Industrial Site (I), Industrial Valley (IV) and inside Industrial site (I). The magnitude of anomalies ($\Delta^{199}\text{Hg}$) found in lichens for each geographical area over the nine years of sampling is represented as a function of the size of the circle.

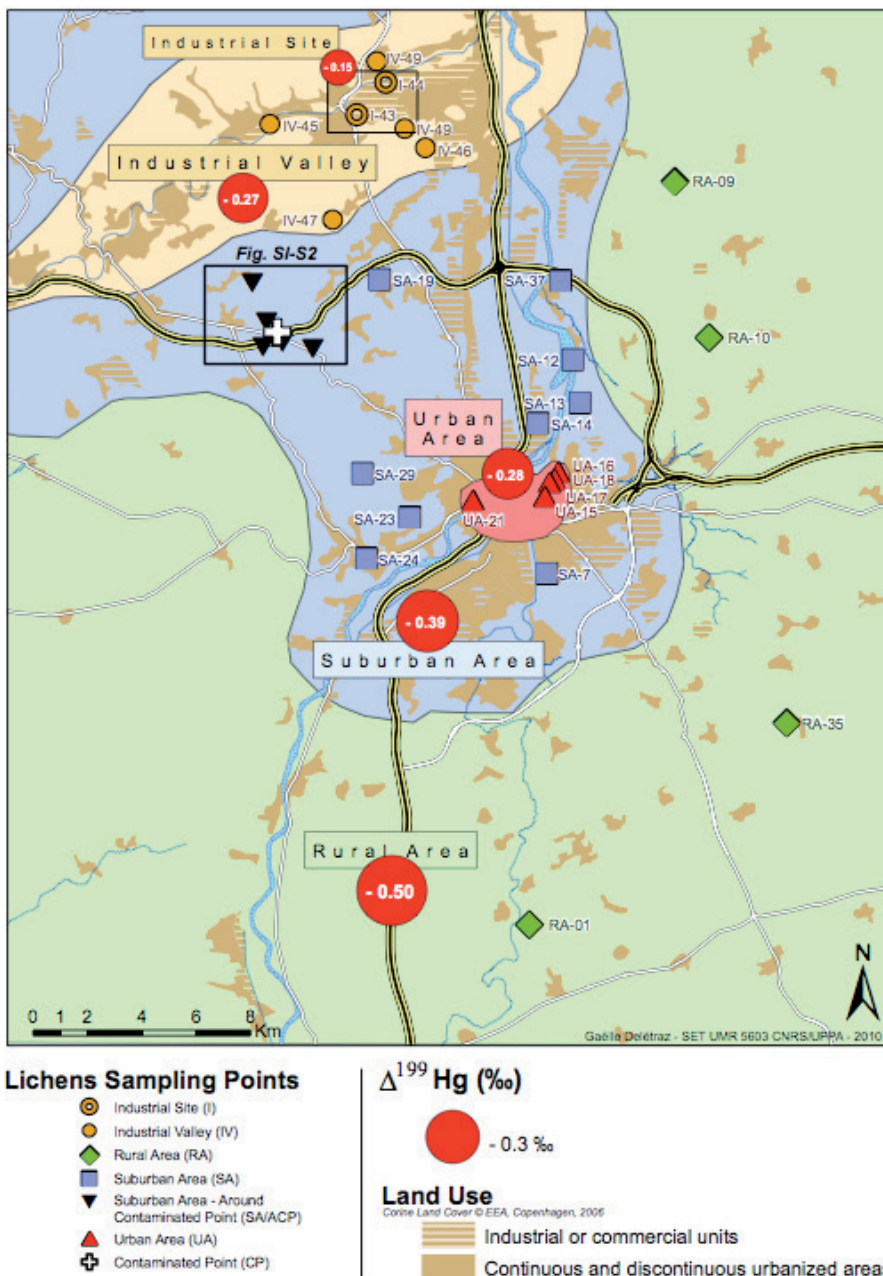


FIGURE SI-S2: Mercury concentrations for each point sampled in Urban Area (UA), Suburban Area (SA), Rural Area (RA), Industrial Valley (IV) and Industrial Sites (I) for the years 2001, 2003, 2006, 2008 and 2009. Lichens species are indicated for each sampling point (see nomenclature in the text above). The horizontal black line and the dotted rectangle represent respectively the average Hg concentration and the standard deviation (SD) on the average within each area.

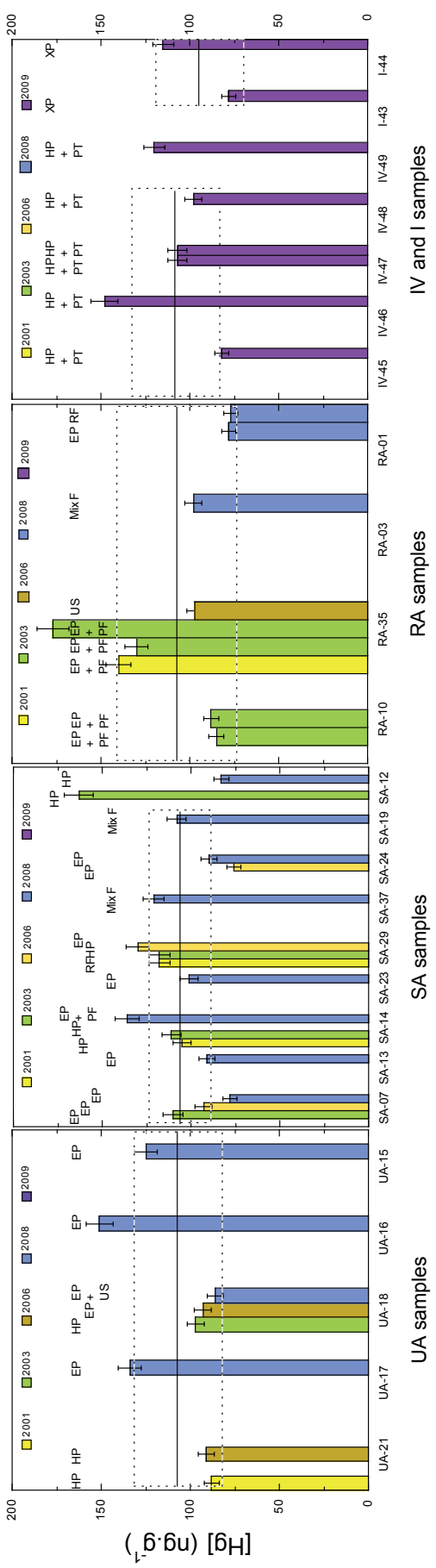


FIGURE SI-S3: $\delta^{202}\text{Hg}$ (‰) for each point sampled in Urban Area (UA), Suburban Area (SA), Rural Area (RA), Industrial Valley (IV) and Industrial Sites (I) for the years 2001, 2003, 2006, 2008 and 2009. Lichens species are indicated for each sampling point (see nomenclature in the text above). The horizontal black line and the dotted rectangle represent respectively the average $\delta^{202}\text{Hg}$ and the 2SE on the average within each area.

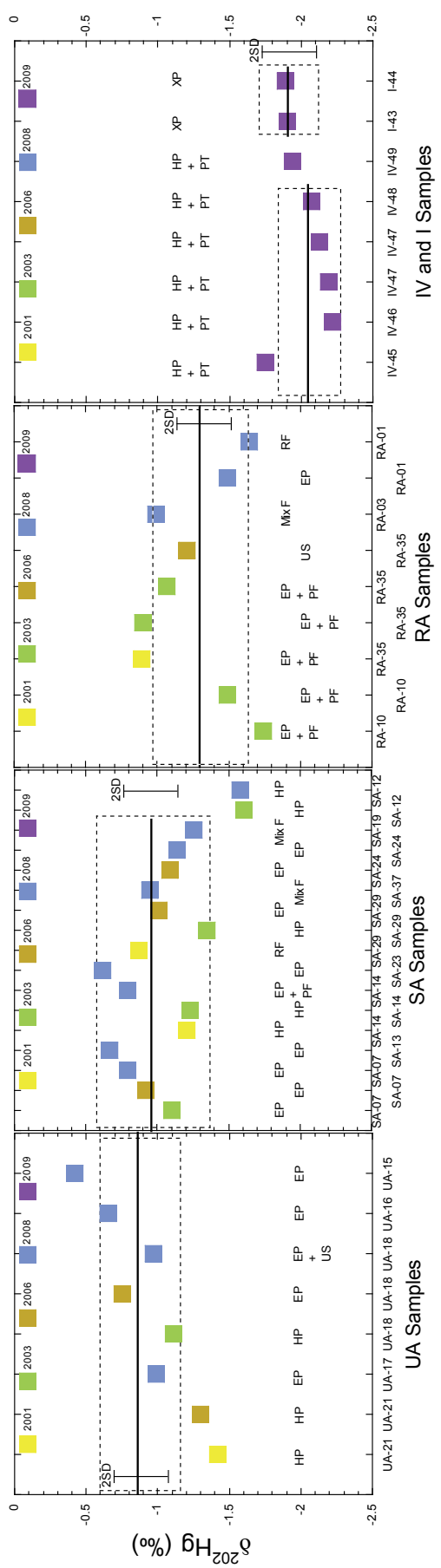


FIGURE SI-S4: $\Delta^{199}\text{Hg}$ (‰) for each point sampled in Urban Area (UA), Suburban Area (SA), Rural Area (RA), Industrial Valley (IV) and Industrial Site: the years 2001, 2003, 2006, 2008 and 2009. Lichens species are indicated for each sampling point (see nomenclature in the text above). The horizontal bar and the dotted rectangle represent respectively the average $\Delta^{199}\text{Hg}$ and the 2SE on the average within each area.

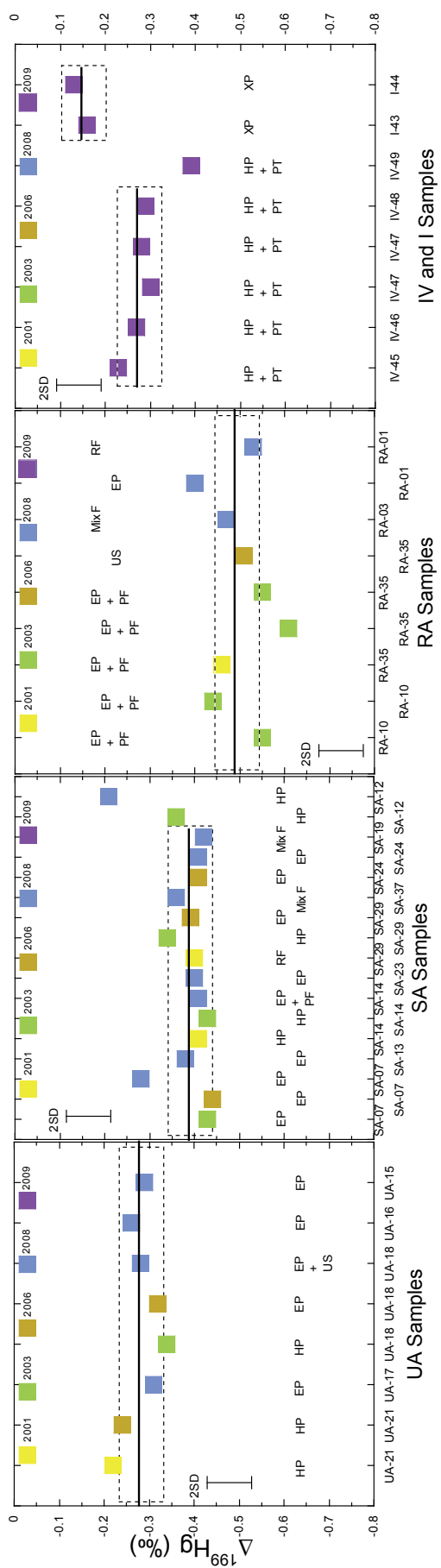


FIGURE SI-S5: Location of the studied area around the contaminated point CP-27

(www.geoportail.fr © 2008 - IGN)

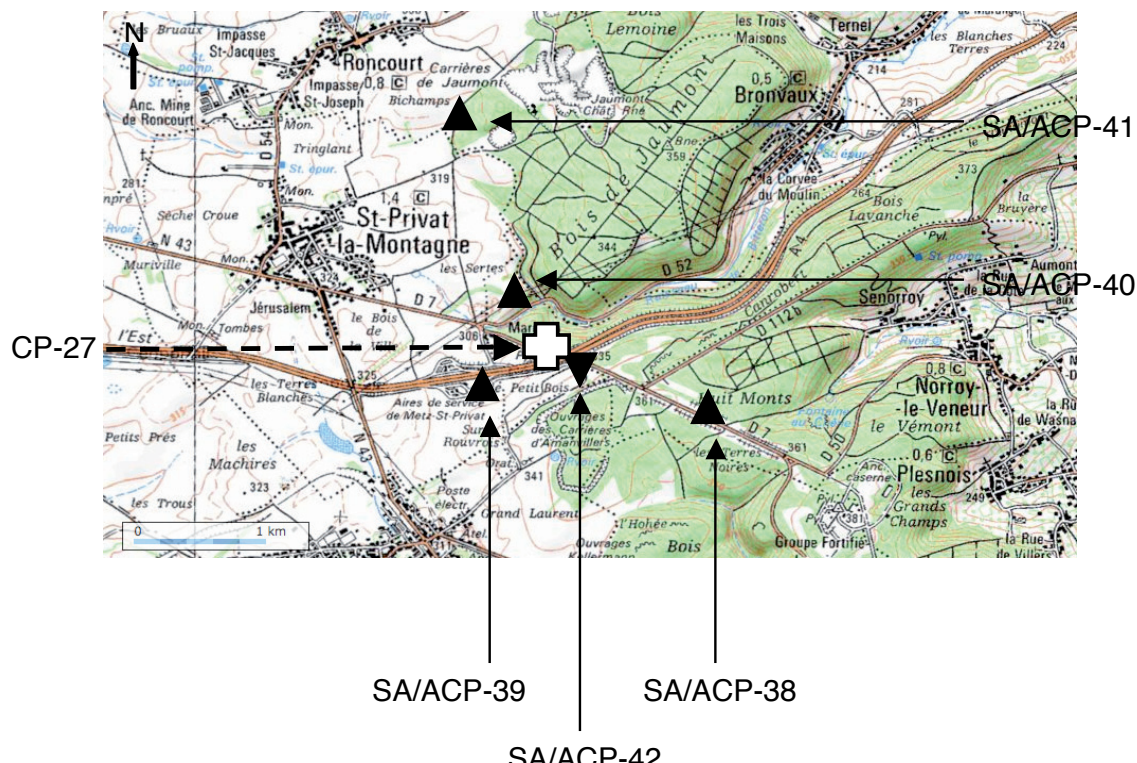


FIGURE SI-S6: Average mercury concentrations (years 2001, 2003, 2006, 2008 and 2009)

for the lichen sampled at the contaminated point (CP-27, empty cross). Lichens sampled around CP-27 (SA/ACP, filled black triangles) are in the Hg concentrations range of all other lichens of the study. Lichen sampled at around 200 meters of CP-27 (inverse filled black triangle) display an intermediate Hg concentration of 200 ng.g^{-1} .

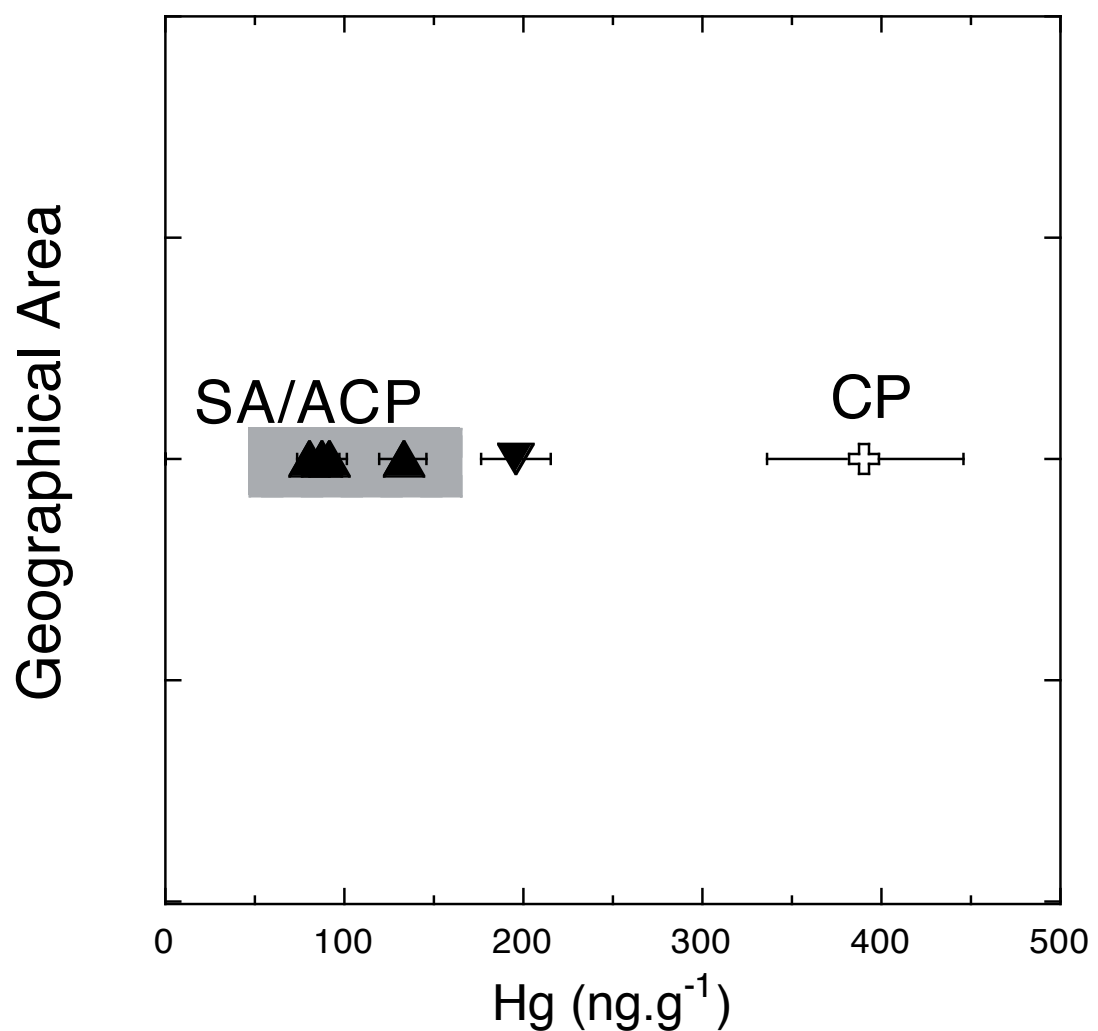
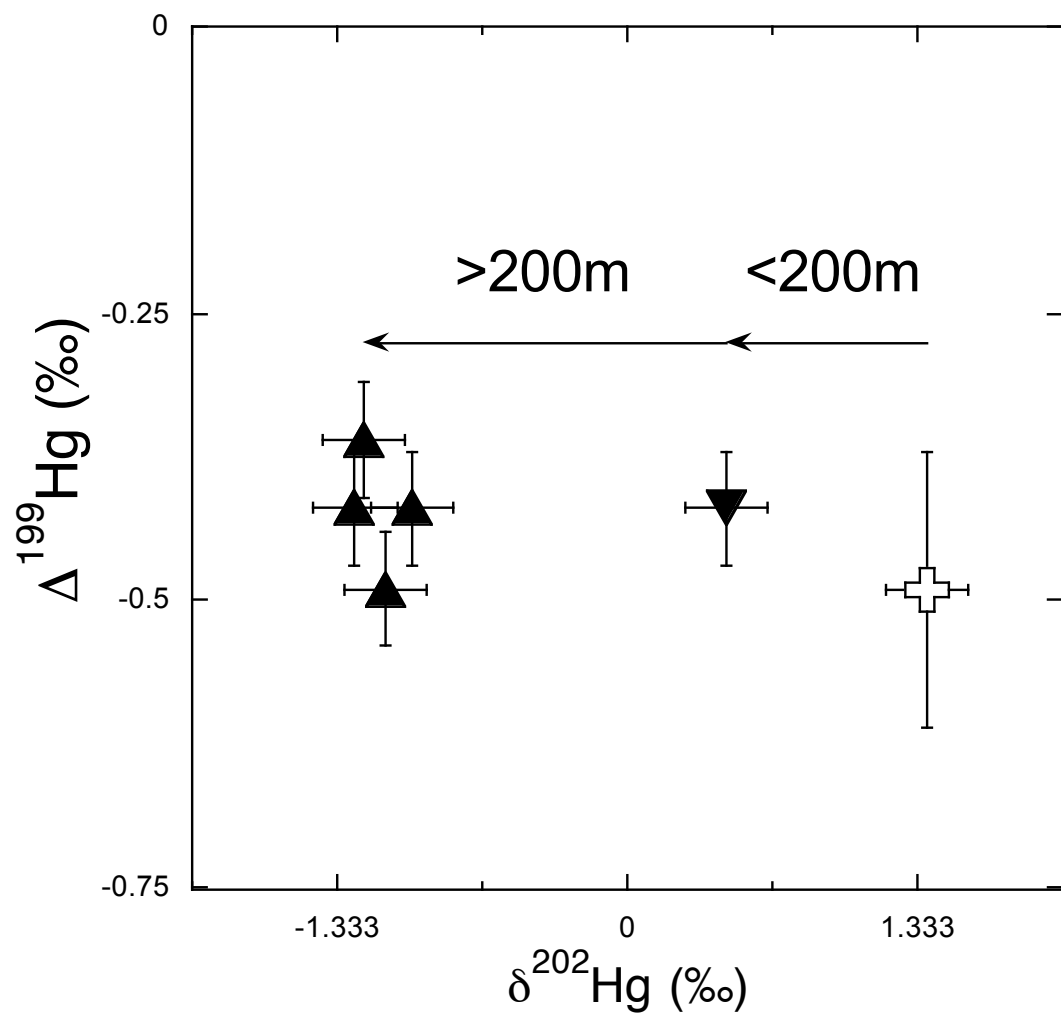


FIGURE SI-S7: $\Delta^{199}\text{Hg}$ versus $\delta^{202}\text{Hg}$ for the lichens sampled at the contaminated point (CP-27, empty cross) in suburban area around the contaminated point (SA/ACP 38-39-40-41, filled black triangles) and at 200 meter of CP-27 (SA/ACP 42, inverse filled black triangles).



Tracing and Quantifying Anthropogenic Mercury Sources in Soils of Northern France Using Isotopic Signatures

Nicolas Estrade,^{*,†,‡} Jean Carignan,[†] and Olivier F. X. Donard[†]

[†]Centre de Recherches Pétrographiques et Géochimiques (CRPG), Nancy-Université, CNRS/INSU, 15 rue Notre-Dame-des-Pauvres B.P. 20 F-54501 Vandœuvre les Nancy, France

[‡]Institut Pluridisciplinaire de Recherche sur l'Environnement et les Matériaux, Laboratoire de Chimie-Analytique Bio-Inorganique et Environnement, Université de Pau et des Pays de l'Adour, CNRS UMR 5254, HELIOPARC, 64053 Pau, France

 Supporting Information

ABSTRACT: The mercury (Hg) isotopic composition was investigated in topsoils from two case studies in north of France. The Hg isotope composition was first determined in agricultural topsoils contaminated by a close by Pb–Zn smelter. The Hg isotopic composition was also measured in topsoils from an urban area in northeastern France (Metz). In both cases, no significant mass independent isotope fractionation could be found in the soils. However, the soil isotopic composition ($\delta^{202}\text{Hg}$) was enriched in the heavier isotopes as the Hg concentration increased in the soils. A linear relationship between the $\delta^{202}\text{Hg}$ in soils and $1/\text{[Hg]}$ indicated a mixing between a contamination source and the Hg derived from the geogenic background soils. Such findings demonstrate that the contamination signature was preserved in the soils and that the deposition of anthropogenic Hg was predominant compared to reactions leading to isotope fractionation such as biotic and abiotic reduction of Hg(II) and resulting in Hg mobility or evasion from the soils. It was therefore possible, for the first time in the case of Hg, to evaluate the contribution of the contamination source relative to the background Hg source in urban topsoils using relative isotope abundances.

INTRODUCTION

Global mercury (Hg) emissions are dominated by anthropogenic sources.¹ Coal combustion represents more than the two-thirds of the total anthropogenic emissions. The rest is represented by various industrial sources.² The unravelling of anthropogenic mercury origin with respect to the natural sources in the environment is the current challenge and of paramount importance. The relative abundance of mercury isotopes may vary during chemical and phase transformations and consequently between various geological and environmental reservoirs.³ Indeed, mercury isotopes present large mass dependent (MDF) and mass independent (MIF) fractionation ranges ($\approx 7\%$ for the $\delta^{202}\text{Hg}$ and $\approx 10\%$ for the $\Delta^{199}\text{Hg}$, respectively) resulting from biophysico-chemical processes taking place either in the natural or the anthropogenic sources independently. However, very few studies have successfully discriminated the anthropogenic mercury sources using its isotopes from background sources and followed its distribution and mixing in the environment.^{4–6}

Anthropogenic Hg originates primarily from Hg ores used for a variety of industrial processes. The cinnabar, metacinnabar, or Hg-bearing ores and fossil fuels present a large range of MDF with little to no MIF^{5,7–10} probably because Hg was affected by various physicochemical reactions (e.g., redox, evaporation–condensation) but little or no photoreactions. Therefore, the various forms and levels of mercury entering the environment through industrial activities probably have little to no MIF signatures¹¹ when compared to those found in surface or subsurface environments such as aquatic systems,^{12–14} atmosphere,^{6,11,15} or in arctic systems.¹⁶ In these later cases, Hg has undergone many biophysico-chemical processes during its cycling before being

stored. The Hg isotopes may also undergo isotopic fractionation during anthropogenic processes (combustion/condensation/precipitation) before being expelled to the environment but no significant MIF were reported to date for such transformations.^{10,17,18}

Among different reservoirs, the terrestrial compartment is both an important source and sink for Hg regarding the atmosphere.¹⁹ Local Hg contamination in soils therefore results mainly from the deposition of the oxidized Hg forms (and/or particulate ones) because Hg^0 displays a very long residence time. Indeed, this Hg^0 is not easily oxidized close to its sources or during transportation and shows little deposition close to the source of emission.^{20,21} In general, primary atmospheric Hg sources to soils are wet and dry deposition. Reemissions of Hg from soils can also be reintroduced to the soils.²²

Once in the soil, Hg undergoes a variety of processes such as adsorption and desorption,²³ precipitation, and volatilization that contributes to its mobility.²⁴ Hg emissions from soils are controlled by a number of processes directly related to environmental parameters and characteristics of the soils and biophysico-chemical processes such as reduction (biotic or abiotic) or photoreduction.²² These mechanisms result in isotopic fractionation leading to MDF^{25–28} or both MDF and MIF.^{12,29–33} The original isotopic signature of Hg contamination may thus be altered with time.

This work aims at evaluating the potential of Hg isotopes fractionation to discriminate anthropogenic from natural

Received: August 6, 2010

Accepted: January 3, 2011

Revised: December 5, 2010

signatures in soils from two different and separate locations in Northern France. These soils are (i) cultivated top soils, contaminated by a close Pb–Zn smelter (ii) top soils originating from an urban area.

MATERIALS AND METHODS

Studied Areas. (i). *Northern France, Soils Contaminated by a Pb–Zn Smelter.* The first site where soils were collected is around a Pb–Zn smelter located in northern France close to the town of Noyelles-Godault. This site was one of the largest Pb–Zn smelters in Europe until 2003 and has been extensively studied. Contamination records of the surrounding environment have been assessed with a time span of more than one hundred years. The soil samples analyzed originate from agricultural ploughed top soils located from one to four kilometers around the smelter in the northern and southern directions. Site and soils description can be found in Sterckeman et al.³⁴ Results reported clearly showed that these soils have been contaminated by the smelter for many trace metal elements such as Cd, Pb, Zn, Ag, As, Bi, Cu, Hg, In, Sb, Sn, and Tl with decreasing concentrations with the distance of the sampling site to the smelter. Furthermore, these soil samples have been previously analyzed by Cloquet et al.^{35,36} for their Cd, Pb, and Zn isotopic composition. Their results clearly highlighted that, on the basis of isotopic signatures, the smelter was the direct contamination source. In order to characterize the emission source, two dust samples from the smelter (sleeved filters before emission to the atmosphere) were analyzed for their Hg concentration and isotopic composition, and one slag sample was analyzed for its Hg concentration only.

(ii). *Northeastern France, City of Metz, Urban Top Soils.* The second site is located in Northeastern France in the urban area of the city of Metz (200000 inhabitants). The area selected for sampling (SI Figure SI–S1) represents a surface of 3 km², bordered on the southwestern side by the city center of Metz, on the southern and eastern sides by the suburban area, and finally on northern and northwestern sides by a commercial and industrial areas, respectively. According to the cadastral emission inventory realized by the Lorraine Air Quality Agency in 2002 for the city of Metz (see the SI), the global atmospheric Hg emission in the studied area was around 17 kg.y⁻¹. The Hg anthropogenic sources are linked to the coal combustion (60% of the emissions), the waste incineration (35% of the emissions), and the nonindustrial uses (e.g., residential heating; 5%). Regarding coal combustion, one power plant using either coal (10%) or gas (90%) (CGFPP, 155 MW) is located on the west-southwestern side of the studied area (SI Figure SI–S1). The CGFPP started its activity in 1961 and was mainly operated as a coal power plant exclusively before its transformation in 1992. Another coal combustion unit of 39 MW is in operation since 1984 and located 2.5 km to the southeast of the studied area (not shown in SI Figure SI–S1). One municipal solid waste incinerator (MSWI) in operation is located on the west-southwestern side of the studied area, nearby the CGFPP (SI Figure SI–S1). The MSWI started its activity in 2001, replacing an old MSWI (1969–1997) located on the same site. About 2 km to the north of the studied area (out of the city of Metz, not shown in SI Figure SI–S1), a large coal fired power plant (CFPP, 500 MW, around 16 kg.y⁻¹ Hg estimated in 2002) is in operation since 1971. Further north, about 10 km from the studied area, is also located an important industrial zone comprising mainly steel industry. However, using Hg isotope signatures in lichens, Estrade et al.⁶ showed that this latter industrial area was

not a significant source of Hg for the urban area studied in this work. Soil samples were collected in July 2008 (see the SI for description). The samples were collected on a top soil surface of 20 cm large, 20 cm long, and 3 cm deep. They were dried, crushed, and sieved by Micropolluants Technologie SA. The soil samples were further crushed at Centre de Recherches Pétrographiques et Géochimiques (CRPG) to a grain size less than 80 µm, used for sample preparation for major, trace elements and isotopic analyses. Major and trace elements concentrations measurements were carried out at CRPG at the Service d'Analyse des Roches et Minéraux (CRPG-SARM³⁷). Mercury concentrations were also performed at CRPG-SARM by using cold-vapor atomic absorption spectrometry (CV-AAS) after hot (100 °C) acidic digestion (HNO₃/H₂SO₄) of 100 mg of soil.

Sample Preparation for Isotopic Analyses. Once crushed, soils, dusts, and slag samples were digested using HNO₃/H₂SO₄ using a sample mass of 1 g as described in Estrade et al.¹⁸ (300 mg only were digested for the dust samples). This sample preparation procedure was also performed on two preparations of the soil reference material NIST-2711 and one preparation of the fly ash reference material BCR-176R. Three soil samples from the city of Metz (urban top soils study) (SJ02, SJ38, SJ47 see Table 1) presenting Hg concentrations of less than 100 ng.g⁻¹ were digested with a high-pressure and high-temperature method as applied to the reference material BCR-482 (High Pressure and High Temperature method - HPA) described in Estrade et al.¹⁸ In this case, 1 g of soil was digested in 3 mL concentrated nitric acid. In order to check on the digestion yields and accuracy of the results, the soil reference material NIST-2711 was also digested and analyzed with this latter set of samples.

Mercury isotopes analyses were performed by cold vapor generation coupled to an MC-ICP-MS Nu Plasma HR (Nu instruments, UK) of the IPREM/LCABIE (Institut Pluridisciplinaire de Recherche sur l'environnement et les Matériaux/Laboratoire de Chimie Analytique Bio Inorganique et Environnement) in Pau. The gas–liquid separator used in this study was the HGX-200 (Cetac, US). Instrumental settings were similar to the ones described in Estrade et al. 2010.¹⁸ Isotopic compositions of the samples are reported in δ values normalized to ¹⁹⁸Hg, as recommended in Blum and Bergquist,³⁸ relative to the NIST SRM 3133 Hg solution as defined for the ^{202/198}Hg ratio

$$\delta^{202/198} (\text{‰}) = \left(\frac{\text{Hg}_{\text{sample}}}{\text{Hg}_{\text{NIST3133}}}^{202/198} - 1 \right) \times 1000$$

Mass independent fractionations measured on the odd ¹⁹⁹Hg and ²⁰¹Hg isotopes are expressed according to the definition of Δ¹⁹⁹Hg (‰) and Δ²⁰¹Hg (‰)

$$\Delta^{199}\text{Hg} (\text{‰}) = \delta^{199}\text{Hg}_{\text{measured}} - 0.252 \times \delta^{202}\text{Hg}_{\text{measured}}$$

$$\Delta^{201}\text{Hg} (\text{‰}) = \delta^{201}\text{Hg}_{\text{measured}} - 0.752 \times \delta^{202}\text{Hg}_{\text{measured}}$$

Acidic matrices of the samples and the reference materials as well as the monoelemental reference material were matched prior to analysis. Isotopic analyses were conducted on sample solutions of 4 ng.mL⁻¹ Hg. The concentrations of samples and of the reference materials were measured prior to isotopic analysis relative to the NIST 3133 in matrix-matched solutions in order to verify digestion yields and to adjust within 5% the sample concentration relative to the NIST 3133. The isotopic composition of a secondary

Table 1. Mercury Concentrations and Isotopic Compositions in Top Soils and Dusts from the Pb–Zn Smelter and Top Soils from the Metz Urban Area

name	location ^a	Hg (ng·g ⁻¹)	n ^b	$\delta^{202}\text{Hg}$ (‰)	2SE	$\Delta^{199}\text{Hg}$ (‰)	2SE	$\Delta^{201}\text{Hg}$ (‰)	2SE
North France: Contaminated Top Soils around the Pb–Zn Smelter									
16b	4291 m (NE)	133	2	−0.90	0.15	−0.04	0.05	−0.02	0.07
17B	2178 m (NE)	193	2	−0.70	0.18	−0.03	0.05	−0.04	0.07
22B	1958 m (NE)	213	2	−0.78	0.15	−0.02	0.08	−0.05	0.07
1B	1746 m (SW)	297	1	−0.77	0.15	−0.04	0.05	−0.09	0.07
52B	1230 m (S)	326	1	−0.62	0.15	0.04	0.05	0.00	0.07
55B	1251 m (SW)	379	2	−0.59	0.15	0.02	0.05	0.02	0.07
36B	891 m (N)	416	2	−0.61	0.15	0.02	0.05	0.03	0.07
32B	1145 m (N)	458	1	−0.59	0.15	0.04	0.05	0.00	0.07
31B	1046 m (N)	489	2	−0.64	0.15	0.05	0.11	−0.02	0.07
34B	990 m (N)	568	2	−0.56	0.15	0.05	0.05	0.05	0.07
30B	954 m (N)	623	2	−0.50	0.15	0.02	0.05	0.07	0.07
Geogenic ^c Hg	Loessic and alluvial soils, 10–20 km	50–70		n.d.	n.d.	n.d.	n.d.	n.d.	n.d.
North France: Industrial Dusts from the Pb–Zn Smelter									
Dust 1	smelter	44200	2	−0.24	0.15	−0.13	0.08	−0.11	0.07
Dust 2	smelter	361000	4	−0.29	0.15	−0.01	0.05	−0.06	0.12
Slag	smelter	<10		n.d.	n.d.	n.d.	n.d.	n.d.	n.d.
Northeastern France, City of Metz: Urban Top Soils									
SJ02*	Metz	40	2	−0.94	0.15	0.07	0.05	−0.01	0.08
SJ38*	Metz	58	1	−0.73	0.15	−0.05	0.05	−0.04	0.07
SJ47*	Metz	80	2	−0.78	0.21	−0.12	0.05	−0.07	0.07
SJ14	Metz	110	2	−0.72	0.16	−0.03	0.05	−0.05	0.07
SJ27	Metz	115	1	−0.60	0.15	−0.07	0.05	−0.05	0.07
SJ12	Metz	120	2	−0.71	0.15	−0.04	0.05	−0.06	0.07
SJ01	Metz	130	1	−0.72	0.15	−0.08	0.05	−0.08	0.07
MC05	Metz	140	2	−0.66	0.15	−0.06	0.06	−0.06	0.07
SJ30	Metz	180	2	−0.43	0.22	−0.05	0.09	−0.05	0.13
MC10	Metz	210	1	−0.45	0.15	−0.08	0.05	0.00	0.07
MB05	Metz	240	1	−0.43	0.15	0.03	0.05	−0.09	0.07
SJ40	Metz	285	2	−0.20	0.19	0.09	0.05	0.06	0.07
SJ52	Metz	330	1	−0.31	0.15	−0.04	0.05	−0.03	0.07
SJ21	Metz	820	1	−0.16	0.15	−0.05	0.05	−0.07	0.07
Reference Materials ^d									
CRPG-F65A		16		−3.50	0.15	0.10	0.05	0.05	0.07
NIST-2711		34520	6	−0.21	0.13	−0.15	0.06	−0.15	0.04
BCR-176R		1470	3	−1.00	0.15	−0.03	0.05	−0.02	0.07

^a Soil location in the Pb–Zn smelter study represents the distance from the Pb–Zn smelter and text in brackets is NE: northeast, N: north, SW: southwest, and S: south. ^b Number of measurements. ^c See text and Sterckeman et al.³⁴ *SJ02, SJ38, and SJ47 were considered as background topsoils (see text), n.d.: nondocumented. ^d The uncertainties are given as 2SD of the n measurements.

monoelemental reference material was measured to determine the external reproducibility of the method. During the course of this study, sixteen measurements of CRPG-F65A led to an isotopic composition of −3.50‰ on the $\delta^{202}\text{Hg}$ in agreement with the published value¹⁸ with a 2 standard deviation from the mean of 0.15‰ (2SD, n = 16) (see Table 1). This value ($\pm 0.15\text{‰}$) is considered as the uncertainty of the method. The uncertainty reported on the samples was 2 standard error of different measurements (2SE). When the 2SE was lower than 0.15‰ or if only one measurement of the sample was performed, the uncertainty of the method was reported. In addition, the isotopic composition of the soil reference material NIST-2711 was measured 6 times for three different preparations including

the High Pressure High Temperature method. Results showed that the isotopic composition of $−0.21 \pm 0.13\text{‰}$ ($\delta^{202}\text{Hg}$, 2SD, n = 6), $−0.15 \pm 0.06\text{‰}$ ($\Delta^{199}\text{Hg}$, 2SD, n = 6), and $−0.15 \pm 0.04\text{‰}$ ($\Delta^{201}\text{Hg}$, 2SD, n = 6) was in agreement with the published value.¹⁸ Three measurements of the fly ash reference material BCR-176R showed a $\delta^{202}\text{Hg}$ of $−1.00 \pm 0.15\text{‰}$ (2SD, n = 3) also in agreement with the published value.¹⁸

RESULTS AND DISCUSSION

Mercury in the Top Soils Contaminated by the Pb–Zn Smelter (Northern France). The concentrations of Hg (Table 1) ranged from 623 ng·g^{−1} at a distance of 954 m from the smelter and dropped down to 133 ng·g^{−1} at 4291 m, the decrease of concentration

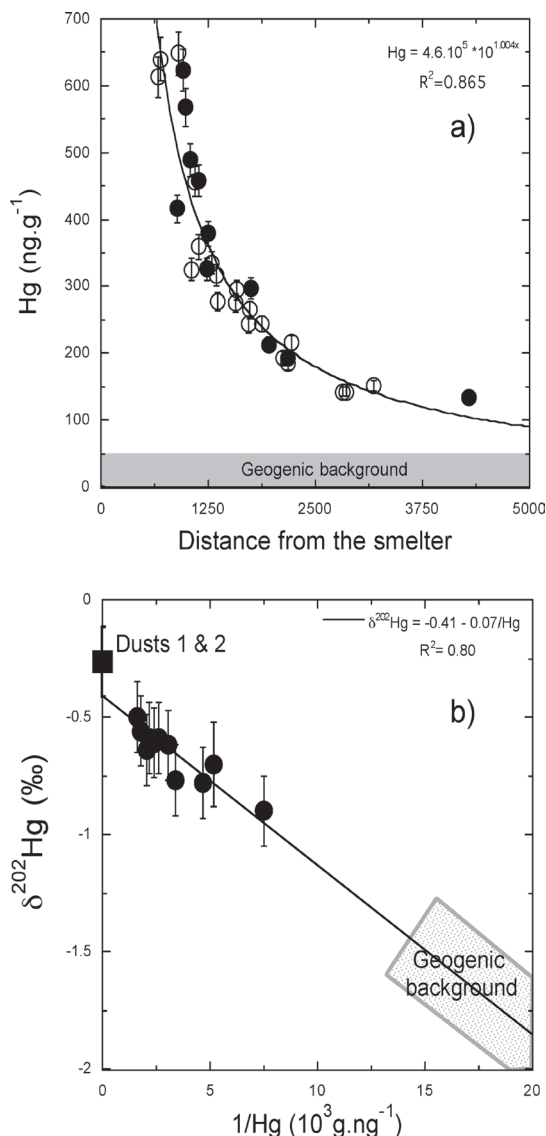


Figure 1. a) Mercury concentrations (ng.g^{-1}) in cultivated top soils in function of the distance (m) from the Zn–Pb smelter. Black empty and black filled circles represent the whole data set analyzed in Sterckeman et al.,³⁴ and only black filled circles samples were analyzed for their isotopic composition in this study. The geogenic background soil Hg concentrations were taken from Sterckeman et al.³⁴ b) $\delta^{202}\text{Hg}$ (‰) of the contaminated top soils samples around the Pb–Zn smelter in function of $1/\text{Hg}$ ($1000 \cdot \text{g.ng}^{-1}$). The linear relationship indicated a mixing between a mercury contamination source and geogenic Hg in soils. Average isotopic composition of two dusts ($\delta^{202}\text{Hg} = -0.29 \pm 0.15 \text{ ‰}$) sampled inside the Pb–Zn smelter fall within error on the linear trend defined by the soil samples.

with the distance from the smelter fits with a power law regression curve (Figure 1a). The same trends were observed for other trace elements (Ag, As, Bi, Cd, Cu, In, Hg, Pb, Sb, Sn, Tl, and Zn) and were interpreted as a result of smelter emissions.³⁴ Soil samples further away from the smelter yielded Hg concentrations ranging between 50 and 70 ng.g^{-1} , and this concentration was interpreted by Sterckeman et al.³⁴ as the natural geogenic background for the whole area. The concentrations recorded in the present study

soil samples displayed Hg enrichments ranging between 2- and 10-fold compared to the background soil concentrations.

The mercury isotopic compositions of the soils are presented in Table 1. In the Supporting Information (SI), Figure SI–S2 presents the soils $\delta^{199}\text{Hg}$ vs $\delta^{202}\text{Hg}$. No significant MIF was recorded or observed in these soils (in SI Figure SI–S3). The sample with the lowest Hg content has also the lowest $\delta^{202}\text{Hg}$ measured value ($-0.90 \pm 0.15 \text{ ‰}$), whereas Hg-rich samples, closer to the smelter, have less negative $\delta^{202}\text{Hg}$ values reaching up to $-0.50 \pm 0.15 \text{ ‰}$. Figure 1b presents the Hg isotopic composition ($\delta^{202}\text{Hg}$) of the soils plotted against $1/\text{[Hg]}$. The data points display an inverse linear relationship ($r^2=0.80$) resulting from a binary mixing. Thus, Hg in the top soils originates from a direct mixing between a Hg contamination source ($1/\text{[Hg]} \rightarrow 0$ and $\delta^{202}\text{Hg}$ of $\sim -0.4 \text{ ‰}$) and the natural and geogenic background soils ($14 < 1/\text{[Hg]} < 20$, corresponding to the Hg background concentrations and $\delta^{202}\text{Hg} \leq 1.5 \text{ ‰}$). As no significant MIF was recorded in these top soils, both Hg sources are free of MIF.

Mercury in the Urban Top Soils of the City of Metz, (Northeastern France). The Hg contents measured in 14 top soil samples in the urban area over a territory of 3 km^2 spanned over a concentration range from 40 to 820 ng.g^{-1} (Table 1). From this sample set, 3 samples displayed concentrations between 40 and 80 ng.g^{-1} , 5 samples between 110 and 140 ng.g^{-1} , 5 samples between 180 and 330 ng.g^{-1} , and only one sample displayed a concentration of 820 ng.g^{-1} . The Hg-poor samples (40 to 80 ng.g^{-1}) were considered as representative of the Hg geogenic background in top soils since the concentrations recorded were in agreement with those generally found in non contaminated soils.¹⁹ Thus, top soil samples with higher mercury contents than the mean background value have Hg enrichment of 3- to 13-fold relative to the geogenic $[\text{Hg}]$ top soils. This strongly suggests heterogeneity of Hg concentration in urban top soils and the occurrence of other sources than the natural geogenic one.

The mercury isotopic compositions determined in these top soils are presented in Table 1. Like for soil samples close to the Pb–Zn smelter, most urban top soils fall within error on the mass fractionation line in a three-isotope plot (in SI Figure SI–S2). Isotopic anomalies in ^{199}Hg and ^{201}Hg ($\Delta^{199}\text{Hg}$ and $\Delta^{201}\text{Hg}$, respectively) were negligible for most samples (in SI Figures SI–S3 and SI–S4). Only one background soil (SJ47) and the sample SJ40 display a significant MIF ($\Delta^{199}\text{Hg} \geq \pm 0.1 \text{ ‰}$). Based on these two data points only, we concluded that it is not relevant to discuss on the slope value (in SI Figure SI–S3) and the sign of the anomaly and its possible relationship to fractionation processes involved.

The $\delta^{202}\text{Hg}$ values measured in the urban top soils ranged from -0.90 to -0.16 ‰ . As for the soils nearby the Pb–Zn smelter (northern France), the $\delta^{202}\text{Hg}$ value is inversely correlated to Hg concentration (Table 1). Indeed, the $\delta^{202}\text{Hg}$ plotted as a function of $1/\text{[Hg]}$ displayed a linear relationship (Figure 2; $r^2=0.89$, background topsoils excluded from the regression, see below). Here again, the Hg isotopic composition in urban top soils strongly suggest the presence of Hg sources having distinct $\delta^{202}\text{Hg}$ values.

The Preservation of Mercury Signature in Soils: Implications for Isotope Source Discrimination. In both studied cases, the isotopic signature recorded in the soils represents and integrates many years of atmospheric depositions. Processes enhancing the mobility of mercury in the soil as well as the ones leading to Hg evasion to the atmosphere must have taken place over this period. Biotic and abiotic reduction or volatilization processes have been documented to fractionate Hg isotopes in a mass dependent

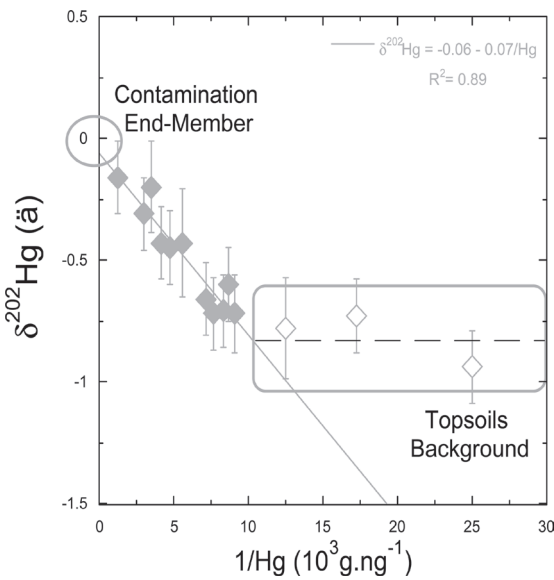


Figure 2. $\delta^{202}\text{Hg}$ (‰) of top soils sampled in the urban area of Metz (Northeastern France) in function of $1/\text{Hg}$ concentration (1000 g.ng^{-1}). The linear relationship observed for samples with $>100 \text{ ng.g}^{-1}$ Hg (filled diamonds) indicated a mixing between a contamination source with an end-member of $\approx -0.05\text{‰}$ ($\delta^{202}\text{Hg}$) and geogenic Hg (open diamonds). The isotopic composition of the background soil was measured in three soils having low Hg content (40 to 80 ng.g^{-1} , empty black diamonds) and displayed a $\delta^{202}\text{Hg}$ of $-0.82 \pm 0.22\text{‰}$ (2SD , $n=3$).

manner.^{25–28} Reduction or photoreduction processes mediated by organic matter have been documented to fractionate Hg isotopes in both mass dependent and mass independent manners.^{12,31–33} In these studies, the $\text{Hg(II)}/\text{Hg}^0$ fractionation factors recorded on the $^{202}/^{198}\text{Hg}$ ratio ($\alpha_{^{202}/^{198}\text{Hg}_{\text{Hg(II)}}/\text{Hg}^0}$) was always lower than 1.002. Hence, as the reduction or photoreduction processes would proceed, the Hg(II) fraction remaining would then decrease and progressively be enriched in the heavier isotopes. The relationships between $[\text{Hg}]$ and $\delta^{202}\text{Hg}$ shown in Figures 1b and 2 contrast with the direction of the isotopic fractionation involved by reduction and photo-reduction processes. Further, the magnitude of the isotopic fractionation ($\alpha_{^{202}/^{198}\text{Hg}_{\text{Hg(II)}}/\text{Hg}^0}$) during these reduction processes is relatively low. For example, using an average $\alpha_{^{202}/^{198}\text{Hg}_{\text{Hg(II)}}/\text{Hg}^0}$ of 1.0015, a significant effect on the isotopic composition of remaining Hg would be detected if more than 20% of total soil Hg(II) would have been reduced to Hg^0 . Photoreduction, reduction, or chemical binding processes have been documented to yield distinct MIF^{12,30–33} resulting in a large fractionation factor range for odd isotopes anomalies ($1.0002 < (\Delta^{199}\text{Hg})_{\text{Hg(II)}}/\text{Hg}^0 < 1.006$). All soil samples analyzed for this study displayed no or very small MIF that could not be related to systematic changes in Hg concentrations and/or $\delta^{202}\text{Hg}$ values. With the data set in hand, we suggest that if any process leading to MIF occurred in the studied soils, it did not alter in a significant manner the mean Hg composition of the soil so that Hg preserved the isotopic fingerprint of the global contamination and geogenic sources.

Discrimination of Hg Sources in the Top Soils Contaminated by the Pb–Zn Smelter (Northern France). The relationship in Figure 1b pointed out a $\delta^{202}\text{Hg}$ of $\sim -0.40\text{‰}$ for the

Hg-rich end-member of the mixing trend. In order to characterize the contamination source, a slag and two dust samples from the smelter were analyzed (Table 1). The slag sample had a very low mercury content and was not analyzed for its isotopic composition. This observation is coherent with the fact that high temperatures ($>1050^\circ\text{C}$) are reached during the smelting processes. Under these conditions, it is very likely that Hg in refined materials was totally volatilized. Therefore, the slag sample was not considered as a specific contamination source as was previously reported for soil cadmium.³⁵ The isotopic compositions of the dust 1 and dust 2 samples (44200 and 361000 ng.g^{-1} Hg respectively) showed similar $\delta^{202}\text{Hg}$ of $-0.24 \pm 0.15\text{‰}$ (2SE, $n=2$) and $-0.32 \pm 0.15\text{‰}$ (2SE, $n=4$) respectively. Although the sample dust 2 did not present any MIF, the dust 1 sample presented a small MIF ($\Delta^{199}\text{Hg}$ of $-0.13 \pm 0.08\text{‰}$, 2SE, $n=2$) (see Figures SI–S2 and S3). According to their $\delta^{202}\text{Hg}$ values, the dusts samples would fit the composition of the contaminated end-member as described by the top soil samples in Figure 1. If we assume that no isotopic fractionation between dusts and fume exhausts (sleeved filters were placed before the fume exhaust) takes place, the dust samples are certainly therefore the best representative materials of the smelter source emissions. The sample dust 1 displaying a small MIF, presented a lower Hg concentration than dust 2 and according to the MIF measured in soils, could only account for a very limited part of the Hg budget in soils. One may ask if these dust samples are representative of the one hundred years of smelting activities in the area. Indeed, Cloquet et al.³⁵ reported that Pb isotopic compositions in these two dust samples were not aligned with the soil trend in a three-isotope plot. This was attributed to the fact that the raw material for refining was originating from various locations during the period of operation and had different Pb isotopic signatures, according to the U/Pb, Th/Pb, and the age of the ore deposit. The Pb isotopic composition of top soils integrated the mean composition of refined ore over the years, probably weighted by the emission flux. In contrast, results obtained on Cd and Zn isotopes in the soils suggested a homogeneity of the raw material during the operating period.^{35,36} Indeed, stable Cd and Zn isotope composition of ore deposits may vary but most published data indicate slight variations around a delta zero value.^{39–42} The isotopic composition of Hg in ore deposits and in Hg-bearing rocks range between -3 to $+1\text{‰}$ (on the $\delta^{202}\text{Hg}$) with no to small MIF^{7,9,10} and an average $\delta^{202}\text{Hg}$ value of -0.65‰ for the whole range of samples analyzed.⁴³ The isotopic composition of dust samples is very similar to this average value suggesting no or little isotopic fractionation of Hg during smelting operations, certainly because of high temperatures and volatilization yields. Thus, we argue that the mean Hg isotopic signature of refined ore may not have changed over the years of operation and that the composition of dust samples well represents that of refinery atmospheric emissions. The fact that top soils define an array pointing to the composition of the dust in Figure 1 also suggest that the isotopic composition of Hg was not altered during atmospheric transport.

Based on the relationship between $\delta^{202}\text{Hg}$ and $1/\text{[Hg]}$ defined by top soils in Figure 1b, it is possible to estimate the isotopic composition of the background geogenic Hg knowing its concentration in soils of the studied area. A $\delta^{202}\text{Hg}$ ranging from -1.3 to -2‰ would correspond to $14 < 1/\text{[Hg]} < 20$ as determined by Sterckeman et al.³⁴ for the local geogenic background. Such $\delta^{202}\text{Hg}$ were not measured here but similar negative values (from -0.76 to -2.5‰) were already reported

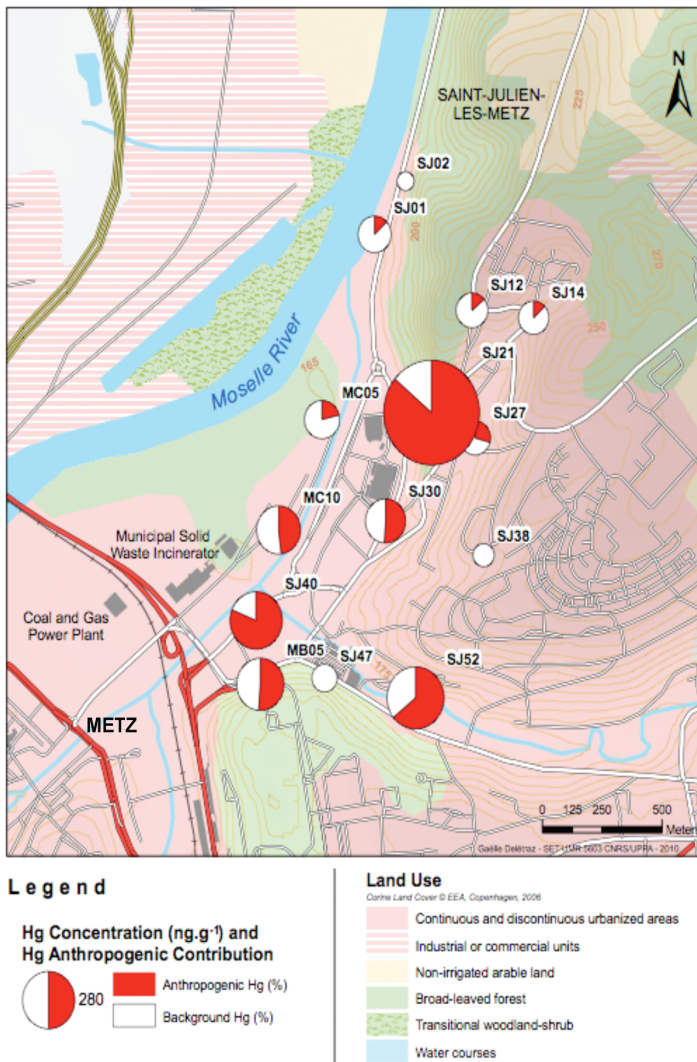


Figure 3. Map of the studied area in the city of Metz (Northeastern France, see text for description) where Hg concentrations (size of the circle) and contribution of anthropogenic Hg (red colored scale, in %, see text) to the soil samples are represented (see map caption).

in the literature for “uncontaminated” sediments and soils (e.g., refs 4, 5, 8, 44). These samples were also free or imprinted of small amount of MIF (<0.4‰). Such MIF compositions are in agreement with the background top soil isotopic compositions suggested here. Furthermore, the $\delta^{202}\text{Hg}$ of geogenic Hg in the literature was shown to be significantly variable between location sites, and a careful investigation should be carried out to accurately quantify the contribution of the anthropogenic source.

Discrimination of the Mercury Sources in Urban Top Soils (City of Metz, Northeastern France). Although the scatter along the trend (Figure 2) may result from various sources having slightly different isotopic compositions, the Hg-rich end member of the mixing is well-defined with a $\delta^{202}\text{Hg}$ of $-0.05\text{\textperthousand}$. This may account for the fact that 1) all pollution sources are well mixed before deposition and 2) only one source is significant, by being more important and/or closer to our sampling sites. According to the fact that our sampling sites display various amounts of Hg “pollution” (over a restricted area), we suggest that the Hg-rich sources are local.

The Hg-poor end-member can be assigned the isotopic composition of background soils with the lowest mercury contents (SJ02, SJ38, and SJ47). Despite a factor of 2 in Hg contents (40, 58, and 80 ng·g⁻¹), these soils presented no significant variation in their isotopic compositions (average $\delta^{202}\text{Hg}$ of $-0.82 \pm 0.22\text{\textperthousand}$, $n = 3$). No relationship between Hg concentrations and the major element chemistry (CaO, Al₂O₃, SiO₂, TOC, not shown here) showing quartz/carbonate or organic matter dilution was identified to explain the [Hg] variation of these three samples. This homogeneous background isotopic composition put these samples slightly off the trend defined by the other samples in Figure 2 and contrasts with our hypothesis on the isotopic composition of geogenic Hg in the other studied area (Northern, France). Nevertheless, homogeneity of the isotopic composition for geogenic Hg at a given site has already been reported in sediments.^{45,44} It appears in this study that background urban top soils display a homogeneous isotopic composition and that deviation from this isotopic composition is due to the contribution of independent sources.

Mercury Source Contributions in Urban Top Soils (City of Metz, Northeastern France). The isotopic variation measured in urban top soils result from a mixture of anthropogenic and geogenic Hg. Considering the contamination source as an atmospheric deposition, Hg is progressively added to soil through the years and mixed with geogenic Hg. Therefore, we can apply a simple isotope mass balance to the system, $\delta^{202}\text{Hg}_{\text{soils}} = X_{\text{cont}}\delta^{202}\text{Hg}_{\text{cont}} + X_{\text{nat}}\delta^{202}\text{Hg}_{\text{nat}}$ where subscripts *cont.* and *nat.* refer to the contamination source and natural source respectively and $X_{\text{cont}} + X_{\text{nat}} = 1$. The fraction of Hg originating from the anthropogenic contamination source (X_{cont}) relative to the fraction of Hg in background soils (X_{nat}) can then be directly evaluated using the isotopic compositions of the two end-members determined above ($\delta^{202}\text{Hg}_{\text{cont}} = -0.05\text{\textperthousand}$ and $\delta^{202}\text{Hg}_{\text{nat}} = -0.82\text{\textperthousand}$). In the soils of the studied area, X_{cont} varies from 0% in background soils to 86% in the most impacted soil. Figure 3 presents the location of the soil-sampling site in the studied area of Metz. The Hg content (size of the circle) associated with the contribution of the anthropogenic end-member (red colored scale, in % relative to the geogenic end-member) are presented in Figure 3. The largest anthropogenic contributions were found on sites centered on the west-southwest side of the studied area, in the valley for MC10 (48%), SJ30 (51%), SJ52 (66%), SJ40 (81%) and down the hill for MB05 (51%) and SJ21 (86%). Samples with a low anthropogenic contribution are found further away in the northeast direction (SJ1, SJ2, SJ12) and on the hill plateau (SJ14, SJ38). The dispersion of the Hg enrichment appeared to be restricted in space suggesting that the anthropogenic contamination did not impact on a large scale and was certainly dispersing from the west-southwest side. When taking into account the main wind direction (SW and NE) and the topography of the studied area, the two mentioned sources of anthropogenic mercury (CGFPP and MSWI) located at the west-southwest side certainly appear as potential contributors to the observed Hg enrichment in top soils.

CGFPP: no data for coal that was used by this plant are available and Hg emission fluxes have not been obtained to date. However according to the literature, Hg emissions from coal combustion flue gas are typically around $10 \mu\text{g.m}^{-3}$, which is considered as an important Hg emitter. Atmospheric Hg related to coal combustion worldwide⁸ should have a normalized to per country emissions $\delta^{202}\text{Hg}$ of $\sim -1.07\text{\textperthousand}$.¹¹ This value is very different from that estimated for the Hg-rich end-member in the studied urban soils as represented in Figure 2 ($\delta^{202}\text{Hg} = -0.05\text{\textperthousand}$). Unless significant isotopic fractionation occurs within the CGFPP during the thermal process, Hg emissions from the CGFPP should not contribute to a large proportion of Hg in the studied urban soils.

MSWI: the total mercury concentrations from the MSWI emissions prior to 1997 were measured at $\sim 100 \mu\text{g.m}^{-3}$. Although this value was below the French standards at this period, the MSWI atmospheric emissions were significant and represented an important Hg source within the urban area. Preliminary results on mercury from the actual MSWI fumes indicate Hg emissions 20- to 50-fold lower than in 1997. Therefore, high Hg concentrations measured in the studied urban soils may have been inherited from the old installation (1969–1997), which undoubtedly emitted larger quantities of Hg to the atmosphere in comparison to the actual MSWI (2001–2008).

Although we showed that Hg isotope tracing is possible in different types of soils, a database for the isotopic composition of Hg emission sources at various scales is still to acquire, to better

constrain relative contributions and establish Hg source budget in soils.

■ ASSOCIATED CONTENT

S Supporting Information. Additional method descriptions and figures. This material is available free of charge via the Internet at <http://pubs.acs.org>.

■ AUTHOR INFORMATION

Corresponding Author

*Phone: +33 559407759. E-mail: nestrade@crpg.cnrs-nancy.fr.

■ ACKNOWLEDGMENT

We would like to thank Thibault Sterckeman for providing the soils from the Pb-Zn Smetler, Christophe Cloquet and Catherine Zimmermann (CRPG) for HPA assistance, Luc Marin and Jitka Lhomme (CRPG-SARM) for their technical support and Sylvain Berail for analytical assistance on the IPREM Nu Plasma. We also address specific acknowledgments to Gaëlle Délétraz at the Laboratoire Société Environnement et Territoire, University of Pau, for map realization and Christophe Cloquet, Jonathan Signoret (Atmolor) and Joe Blum for helpful discussions on the manuscript. This work was supported by an ADEME/BRGM grant. This work was partly funded by HAGANIS, the public institution in charge of the MSWI in Metz and by CNRS EC2CO program (BIOMELI project). This is the CRPG contribution N°2092.

■ REFERENCES

- (1) Lindberg, S.; Bullock, R.; Ebinghaus, R.; Engstrom, D.; Feng, X. B.; Fitzgerald, W.; Pirrone, N.; Prestbo, E.; Seigneur, C. A synthesis of progress and uncertainties in attributing the sources of mercury in deposition. *Ambio* **2007**, *36* (1), 19–32.
- (2) Pacyna, E. G.; Pacyna, J. M.; Steenhuisen, F.; Wilson, S. Global anthropogenic mercury emission inventory for 2000. *Atmos. Environ.* **2006**, *40* (22), 4048–4063.
- (3) Bergquist, B. A.; Blum, J. D. The odds and evens of mercury isotopes: applications of mass-dependent and mass-independent isotope fractionation. *Elements* **2009**, *5* (6), 353–357.
- (4) Foucher, D.; Ogrinc, N.; Hintelmann, H. Tracing mercury contamination from the Idrija mining region (Slovenia) to the gulf of Trieste using Hg isotope ratio measurements. *Environ. Sci. Technol.* **2009**, *43* (1), 33–39.
- (5) Feng, X. B.; Foucher, D.; Hintelmann, H.; Yan, H. Y.; He, T. R.; Qiu, G. L. Tracing mercury contamination sources in sediments using mercury isotope compositions. *Environ. Sci. Technol.* **2010**, *44* (9), 3363–3368.
- (6) Estrade, N.; Carignan, J.; Donard, O. F. X. Isotope tracing of atmospheric mercury sources in an urban area of northeastern France. *Environ. Sci. Technol.* **2010**, *44* (16), 6062–6067.
- (7) Smith, C. N.; Kesler, S. E.; Klaue, B.; Blum, J. D. Mercury isotope fractionation in fossil hydrothermal systems. *Geology* **2005**, *33* (10), 825–828.
- (8) Biswas, A.; Blum, J. D.; Bergquist, B. A.; Keeler, G. J.; Xie, Z. Q. Natural mercury isotope variation in coal deposits and organic soils. *Environ. Sci. Technol.* **2008**, *42* (22), 8303–8309.
- (9) Smith, C. N.; Kesler, S. E.; Blum, J. D.; Rytuba, J. J. Isotope geochemistry of mercury in source rocks, mineral deposits and spring deposits of the California Coast Ranges, USA. *Earth Planet. Sci. Lett.* **2008**, *269* (3–4), 398–406.
- (10) Stetson, S. J.; Gray, J. E.; Wanty, R. B.; Macalady, D. L. Isotopic variability of mercury in ore, mine-waste calcine, and leachates of mine-waste

- calcine from areas mined for mercury. *Environ. Sci. Technol.* **2009**, *43* (19), 7331–7336.
- (11) Carignan, J.; Estrade, N.; Sonke, J. E.; Donard, O. F. X. Odd isotope deficits in atmospheric Hg measured in lichens. *Environ. Sci. Technol.* **2009**, *43* (15), 5660–5664.
- (12) Bergquist, B. A.; Blum, J. D. Mass-dependent and -independent fractionation of Hg isotopes by photoreduction in aquatic systems. *Science* **2007**, *318* (5849), 417–420.
- (13) Gantner, N.; Hintelmann, H.; Zheng, W.; Muir, D. C. Variations in stable isotope fractionation of Hg in food webs of arctic lakes. *Environ. Sci. Technol.* **2009**, *43* (24), 9148–9154.
- (14) Senn, D. B.; Chesney, E. J.; Blum, J. D.; Bank, M. S.; Maage, A.; Shine, J. P. Stable isotope (N , C , Hg) study of methylmercury sources and trophic transfer in the northern gulf of Mexico. *Environ. Sci. Technol.* **2010**, *44* (5), 1630–1637.
- (15) Ghosh, S.; Xu, Y. F.; Humayun, M.; Odom, L. Mass-independent fractionation of mercury isotopes in the environment. *Geochem. Geophys. Geosyst.* **2008**, 9.
- (16) Sherman, L. S.; Blum, J. D.; Johnson, K. P.; Keeler, G. J.; Barres, J. A.; Douglas, T. A. Mass-independent fractionation of mercury isotopes in Arctic snow driven by sunlight. *Nat. Geosci.* **2010**, *3* (3), 173–177.
- (17) Estrade, N.; Carignan, J.; Sonke, J.; Donard, O. F. X. Mass independent fractionation of Hg isotopes during evaporation and condensation processes. *Geochim. Cosmochim. Acta* **2007**, *71* (15), A262–A262.
- (18) Estrade, N.; Carignan, J.; Sonke, J. E.; Donard, O. F. X. Measuring Hg isotopes in bio-geo-environmental reference materials. *Geostand. Geoanal. Res.* **2010**, *34* (1), 79–93.
- (19) Selin, N. E. Global biogeochemical cycling of mercury: a review. *Annu. Rev. Env. Resour.* **2009**, *34*, 43–63.
- (20) Schroeder, W. H.; Munthe, J. Atmospheric mercury - An overview. *Atmos. Environ.* **1998**, *32* (5), 809–822.
- (21) Biester, H.; Muller, G.; Scholer, H. F. Binding and mobility of mercury in soils contaminated by emissions from chlor-alkali plants. *Sci. Total Environ.* **2002**, *284* (1–3), 191–203.
- (22) Schluter, K. Review: evaporation of mercury from soils. An integration and synthesis of current knowledge. *Environ. Geol.* **2000**, *39* (3–4), 249–271.
- (23) Schuster, E. The behavior of mercury in the soil with special emphasis on complexation and adsorption processes - a review of the literature. *Water, Air, Soil Pollut.* **1991**, *56*, 667–680.
- (24) Gabriel, M. C.; Williamson, D. G. Principal biogeochemical factors affecting the speciation and transport of mercury through the terrestrial environment. *Environ. Geochim. Health* **2004**, *26* (4), 421–434.
- (25) Krитеe, K.; Blum, J. D.; Johnson, M. W.; Bergquist, B. A.; Barkay, T. Mercury stable isotope fractionation during reduction of Hg(II) to Hg(0) by mercury resistant microorganisms. *Environ. Sci. Technol.* **2007**, *41* (6), 1889–1895.
- (26) Krитеe, K.; Blum, J. D.; Barkay, T. Mercury stable isotope fractionation during reduction of Hg(II) by different microbial pathways. *Environ. Sci. Technol.* **2008**, *42* (24), 9171–9177.
- (27) Yang, L.; Sturgeon, R. Isotopic fractionation of mercury induced by reduction and ethylation. *Anal. Bioanal. Chem.* **2009**, *393* (1), 377–385.
- (28) Zheng, W.; Foucher, D.; Hintelmann, H. Mercury isotope fractionation during volatilization of Hg(0) from solution into the gas phase. *J. Anal. Atom. Spectrom.* **2007**, *22* (9), 1097–1104.
- (29) Estrade, N.; Carignan, J.; Sonke, J. E.; Donard, O. F. X. Mercury isotope fractionation during liquid-vapor evaporation experiments. *Geochim. Cosmochim. Acta* **2009**, *73* (10), 2693–2711.
- (30) Wiederhold, J. G.; Cramer, C. J.; Daniel, K.; Infante, I.; Bourdon, B. K.; Kretzschmar, R. Equilibrium mercury isotope fractionation between dissolved Hg(II) species and thiol-bound Hg. *Environ. Sci. Technol.* **2010**, *44* (11), 4191–4197.
- (31) Zheng, W.; Hintelmann, H. Mercury isotope fractionation during photoreduction in natural water is controlled by its Hg/DOC ratio. *Geochim. Cosmochim. Acta* **2009**, *73* (22), 6704–6715.
- (32) Zheng, W.; Hintelmann, H. Isotope Fractionation of Mercury during its photochemical reduction by low-molecular-weight organic compounds. *J. Phys. Chem. A* **2010**, *114* (12), 4246–4253.
- (33) Zheng, W.; Hintelmann, H. Nuclear field shift effect in isotope fractionation of mercury during abiotic reduction in the absence of light. *J. Phys. Chem. A* **2010**, *114* (12), 4238–4245.
- (34) Sterckeman, T.; Douay, F.; Proix, N.; Fourrier, H.; Perdrix, E. Assessment of the contamination of cultivated soils by eighteen trace elements around smelters in the North of France. *Water, Air, Soil Pollut.* **2002**, *135* (1–4), 173–194.
- (35) Cloquet, C.; Carignan, J.; Libourel, G.; Sterckeman, T.; Perdrix, E. Tracing source pollution in soils using cadmium and lead isotopes. *Environ. Sci. Technol.* **2006**, *40* (8), 2525–2530.
- (36) Cloquet, C.; Carignan, J.; Lehmann, M. F.; Vanhaecke, F. Variation in the isotopic composition of zinc in the natural environment and the use of zinc isotopes in biogeosciences: a review. *Anal. Bioanal. Chem.* **2008**, *390* (2), 451–463.
- (37) Carignan, J.; Hild, P.; Mevelle, G.; Morel, J.; Yeghicheyan, D. Routine analyses of trace elements in geological samples using flow injection and low pressure on-line liquid chromatography coupled to ICP-MS: a study of reference materials BR, DR-N, UB-N, AN-G and GH. *Geostand. Newslett.* **2001**, *25* (2–3), 187–198.
- (38) Blum, J. D.; Bergquist, B. A. Reporting of variations in the natural isotopic composition of mercury. *Anal. Bioanal. Chem.* **2007**, *388* (2), 353–359.
- (39) Wombacher, F.; Rehkamper, M.; Mezger, K.; Munker, C. Stable isotope compositions of cadmium in geological materials and meteorites determined by multiple-collector ICPMS. *Geochim. Cosmochim. Acta* **2003**, *67*, 4639–4654.
- (40) Cloquet, C.; Rouxel, O.; Carignan, J.; Libourel, G. Natural Cadmium isotopic variations in eight Geological reference Materials (NIST 2711, BCR 176, GSS 1, GXR 1, GXR 2, GSD 12, Nod P1, Nod A1) and anthropogenic samples, measured by MC-ICP MS. *Geostand. Geoanal. Res.* **2005**, *29*, 95–106.
- (41) Wilkinson, J. J.; Weiss, D. J.; Mason, T. F. D.; Coles, B. J. Zinc isotope variation in hydrothermal systems: preliminary evidence from the Irish midlands ore field. *Econ. Geol.* **2005**, *100*, 583–590.
- (42) Sonke, J. E.; Sivry, Y.; Viers, J.; Freydier, R.; Dejonghe, L.; Andre, L.; Aggarwal, J. K.; Fontan, F.; Dupre, B. Historical variations in the isotopic composition of atmospheric zinc deposition from a zinc smelter. *Chem. Geol.* **2008**, *252*, 145–157.
- (43) Yin, R. S.; Feng, X. B.; Shi, W. F. Application of the stable-isotope system to the study of sources and fate of Hg in the environment: A review. *Appl. Geochim.* **2010**, *25* (10), 1467–1477.
- (44) Gehrke, G. E.; Blum, J. D.; Meyers, P. A. The geochemical behavior and isotopic composition of Hg in mid-Pleistocene western Mediterranean sapropel. *Geochim. Cosmochim. Acta* **2009**, *73* (6), 1651–1665.
- (45) Carpi, A. Mercury from combustion sources: A review of the chemical species emitted and their transport in the atmosphere. *Water, Air, Soil Pollut.* **1997**, *98*, 241–254.

1 Supporting Information

2 Tracing and Quantifying Anthropogenic Mercury

3 Sources in Soils of Northern France Using Isotopic

4 Signatures

5 *Nicolas Estrade, Jean Carignan and Olivier F.X. Donard*

6

7 6 pages (including title page)

8 4 Figures (SI-S1 to SI-S4)

9 **Additional description of urban top soil samples in the city of Metz (Northeastern**
10 **France)**

11 Cadastral Hg emission inventory: The inventory of the emission sources of mercury
12 for the city of Metz is documented by the public institution in charge of the air quality in the
13 Lorraine Region (Association de surveillance de la qualité de l'air. www.atmolor.org).
14 Cadastral data are calculated using the combination of the raw flux of each activity division
15 and the emission factors associated with the activity. Methodological guide used for the
16 calculations can be found:

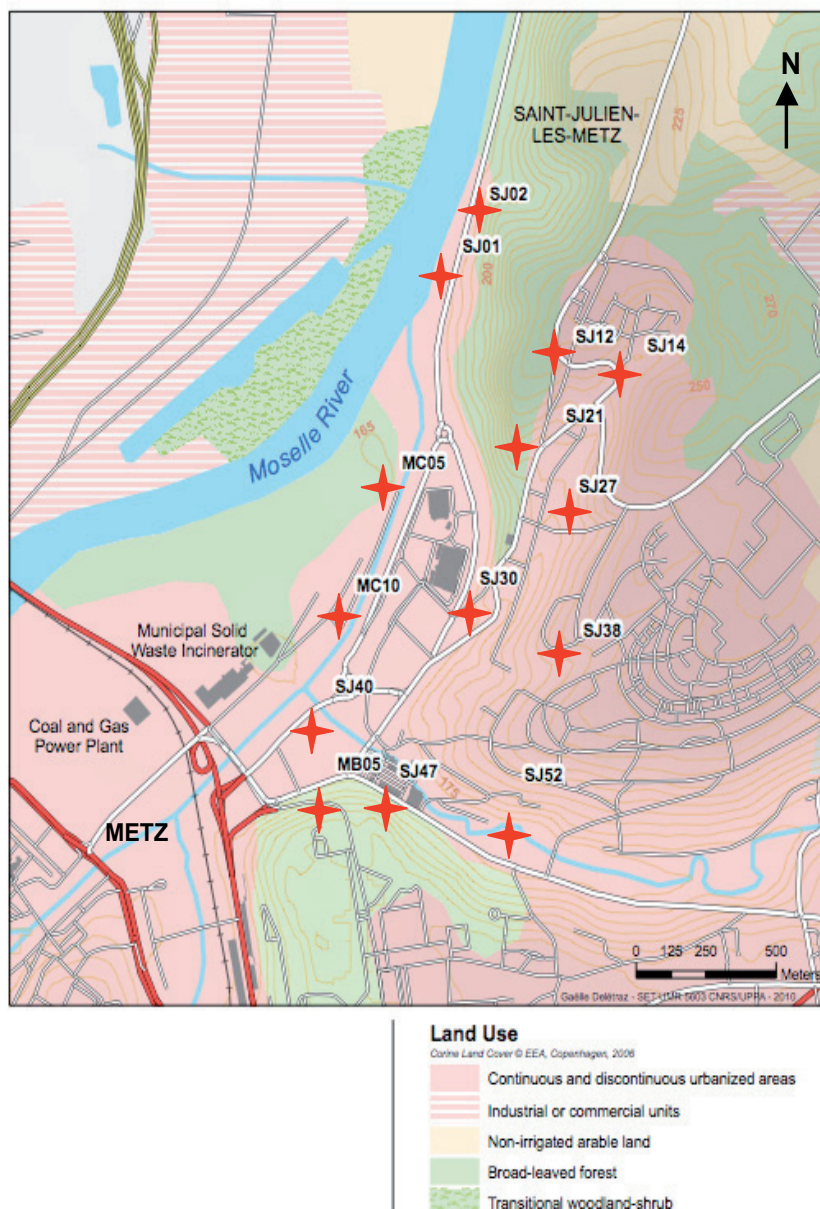
17 http://www.atmo-alsace.net/medias/fichiers/Methologie_inventaire_V2006.pdf.

18 Regarding the city of Metz, the inventory was done with the available data for the year
19 2002.

20 Land use: All soils sampled are free of regular use such as gardening or municipal
21 reworking. Soils were sampled in grass fields, for example along small roads, school
22 backwards, parks and beside trails along small woods. No site was reworked since at least 10
23 years because most were already sampled in 2000 for establishing reference values of metal
24 concentrations in soils of the city of Metz. The average and median Hg concentration in the
25 2000 samples are very similar to that obtained for the 2008 samples suggesting no major
26 change of the Hg atmospheric deposition for the last 10 years."

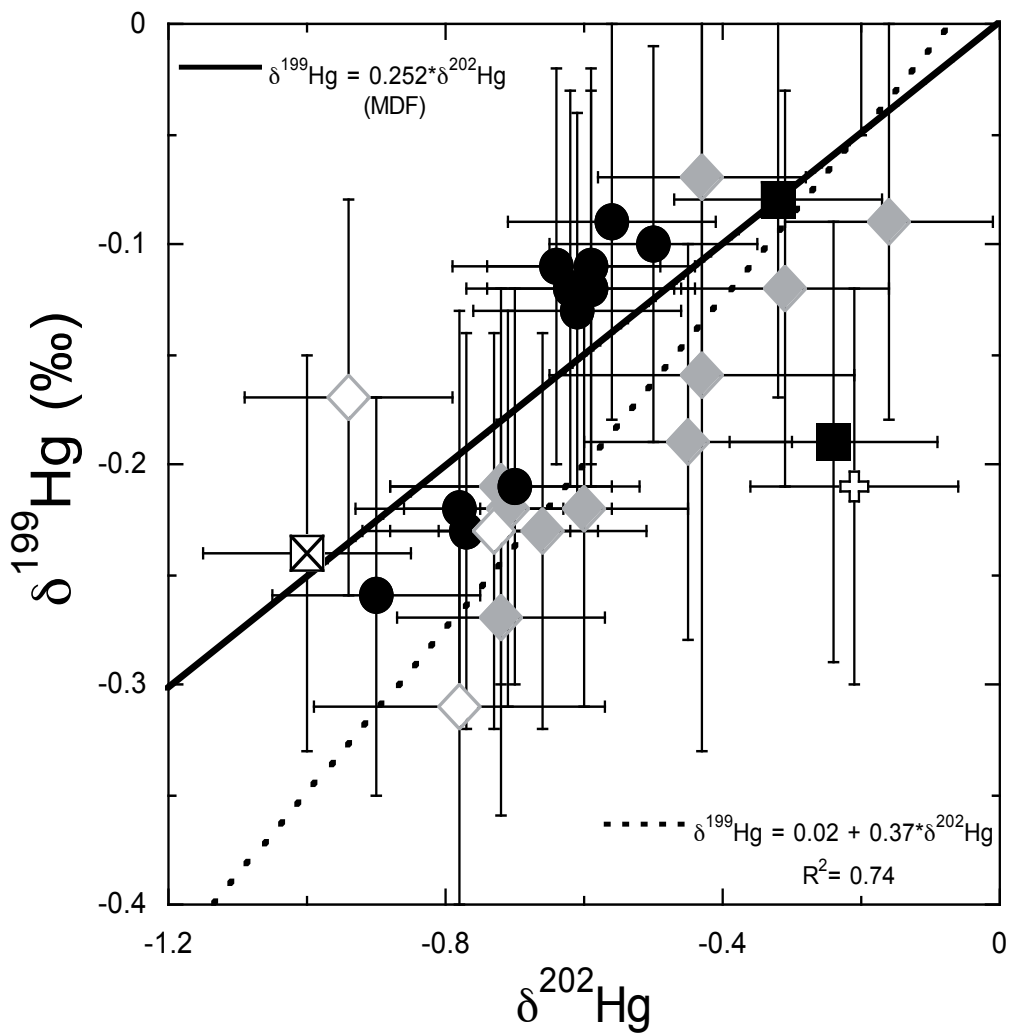
27

28 Figure SI-S1: Map of the studied area in the urban area of the city of Metz (Northeastern
29 France) where the 14 sampling sites, elevation curves and land uses are represented. Sample
30 points are located 1) in valleys along rivers: SJ40 (166m), MC10 (165m), MC05 (165m),
31 SJ01 (168m) SJ02 (170m), SJ52 (170m), SJ30 (168m), 2) down the hill SJ47 (175m), SJ21
32 (190m), MB05 (195m) and 3) on the plateau: SJ27 (210m), SJ38 (215m), SJ14 (220m), SJ12
33 (230m). The CGFPP and the MSWI are located on the southwest corner within the valley at
34 an altitude of 165m. Both chimneys have a height of 35m.

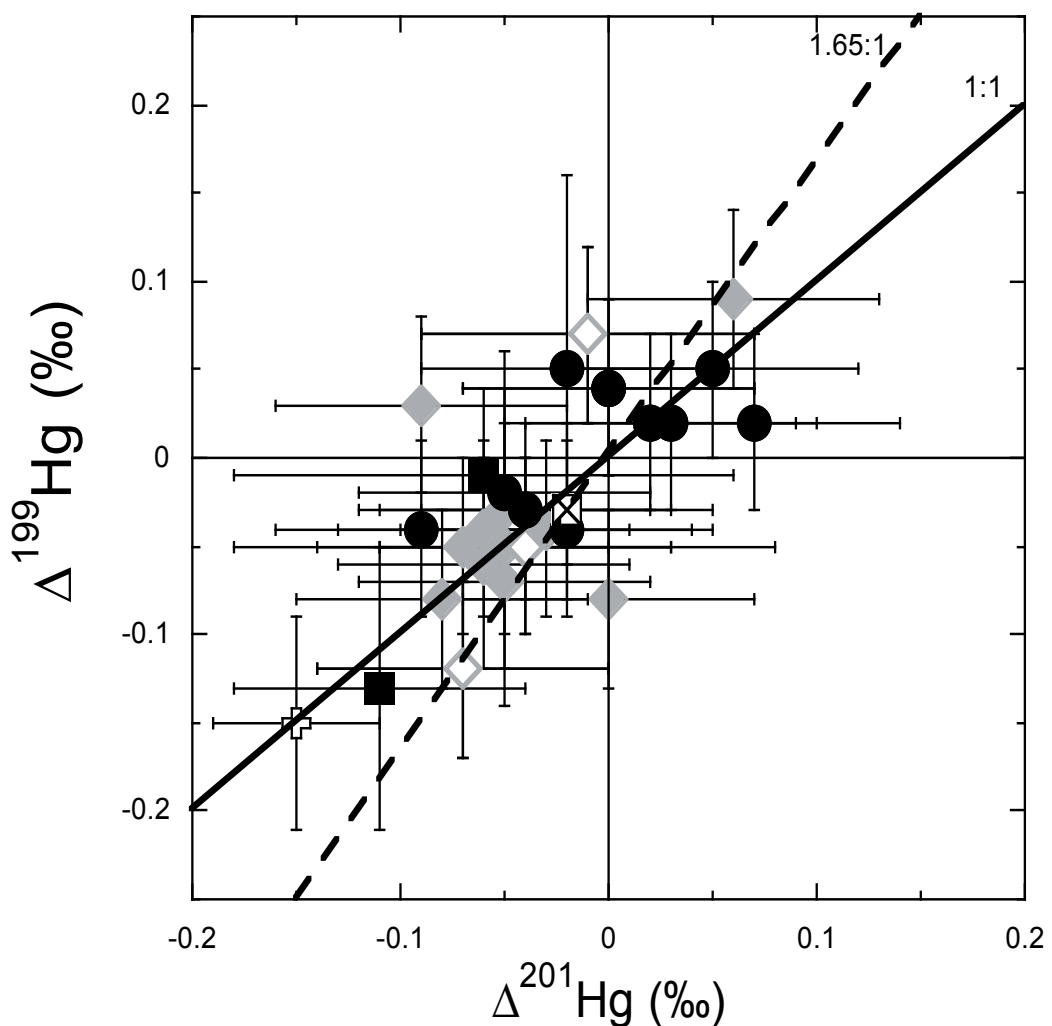


35 Figure SI-S2: Three-isotope diagram where the $\delta^{199}\text{Hg}$ (‰) is plotted as a function of the
36 $\delta^{202}\text{Hg}$ (‰) for all the samples measured in this study: soil reference material NIST-2711
37 (open plus sign), fly ash reference material BCR-176R (square filled with cross), soils around
38 the Pb-Zn smelter (filled circles), dusts from the Zn-Pb smelter (filled squares), soils from
39 Metz in north-eastern France (grey diamonds) and urban background soils from Metz in
40 north-eastern France (open diamonds).

41

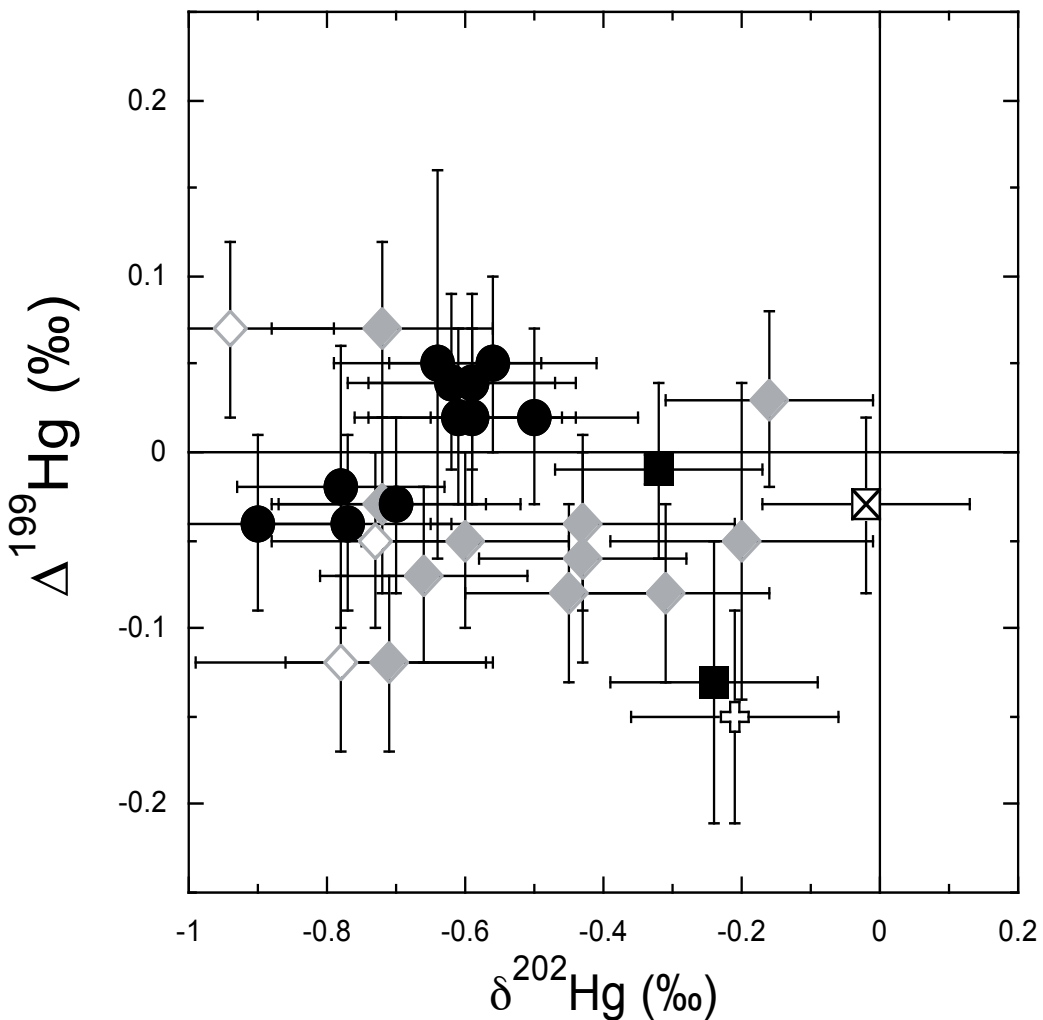


42 Figure SI-S3: $\Delta^{199}\text{Hg} (\text{\textperthousand})$ against $\Delta^{201}\text{Hg} (\text{\textperthousand})$ (symbols as Fig. SI-S2). The 1:1 and the 1.65:1
43 lines correspond to empirical ratios that characterize isotope fractionation related to magnetic
44 isotope effect and nuclear field shift effect respectively.



45 Figure SI-S4: $\Delta^{199}\text{Hg}$ (‰) against $\delta^{202}\text{Hg}$ (‰) (symbols as Fig. SI-S2). This diagram shows
46 that there is no significant relationship between $\delta^{202}\text{Hg}$ and $\Delta^{199}\text{Hg}$ in the soils of the city of
47 Metz.

48



Conclusion & Perspectives



Ce chapitre revient sur les trois grandes parties de ce travail de thèse: l'analyse isotopique, la documentation des facteurs de fractionnement isotopique et l'utilisation des isotopes du mercure pour discriminer et tracer les sources anthropiques dans l'environnement. Il présente pour chaque partie les concepts scientifiques utilisés, les résultats apportés ainsi que les perspectives entrevues.

- L'analyse isotopique du mercure

La technique analytique mise en œuvre dans ce travail est basée sur un système d'introduction du mercure en phase gazeuse couplé à un ICP-MS multicollecteur. Le système d'introduction utilisé est la génération de vapeurs froides de Hg⁰ par une réduction du Hg(II) avec un réducteur puissant (SnCl₂).

Cette technique requiert une étape préalable de traitement de l'échantillon afin de mettre en solution la totalité du mercure d'une matrice minérale ou organique. Les méthodes de mises en solutions disponibles dans la littérature sont nombreuses. Néanmoins celles-ci dépendent principalement du type d'échantillon et de la concentration minimum nécessaire pour réaliser l'analyse isotopique. La méthode haute pression et haute température appliquée à de nombreux échantillons dans ce travail a permis d'analyser des matériaux de compositions chimiques variées contenant au minimum 30 ng.g⁻¹ de Hg en introduisant plus d'un gramme d'échantillon dans seulement quelques millilitres d'acide concentré. Les rendements de digestion de cette technique sont généralement très élevés, mais cette méthode nécessite davantage de temps que des attaques plus modérées.

L'intérêt majeur de la technique de génération de vapeurs froides est de séparer en ligne le Hg⁰ de la matrice. Cette séparation du Hg⁰ de la matrice permet d'abord d'introduire l'échantillon sous forme gazeuse. Ceci évite la désolvatation de l'analyte dans le plasma et augmente ainsi la sensibilité par rapport à une analyse liquide. Cette technique permet également de s'affranchir des interférences potentielles de la matrice sur le biais de masse lors d'analyses d'échantillons avec des matrices chargées en éléments majeurs et traces. Cela permet donc d'obtenir des variations de biais de masse faibles entre les échantillons et les matériaux de références généralement préparés dans des matrices plus simples. C'est une technique d'introduction simple et robuste. Cependant, elle nécessite dans tous les cas de vérifier les rendements de réduction des échantillons par rapport aux matériaux de référence lors de l'analyse de nouveaux échantillons, ou de nouvelles matrices, afin d'éviter des fractionnements non désirés liés à la réduction du mercure.

La mesure des compositions isotopiques a été réalisée par la méthode de l'encadrement de l'échantillon par un matériau de référence («sample standard bracketing» en anglais)

associée à une correction des variations du biais de masse instrumental par mesure simultanée du rapport isotopique $^{205/203}\text{Tl}$ certifié isotopiquement (NIST 997). La loi de correction utilisée est la loi exponentielle. Cette technique de mesure est à l'heure actuelle la plus utilisée au sein de la communauté des isotopistes du mercure.

Les performances analytiques de cette méthodologie ont permis d'analyser la composition isotopique d'échantillons avec seulement 10ng de mercure et d'obtenir des reproducibilités externes (2SD) de l'ordre de 0.15 à 0.25% sur le rapport $^{202/198}\text{Hg}$ et de l'ordre de 0.05% sur les anomalies $\Delta^{199}\text{Hg}$ et $\Delta^{201}\text{Hg}$.

Dans ce travail, nous avons caractérisé près d'une dizaine de matériaux de référence ainsi que deux matériaux de référence mono élémentaires secondaires isotopiquement fractionnés et maintenant disponibles pour la communauté scientifique. Cette dizaine de matériaux de référence caractérisée s'ajoute à la dizaine déjà caractérisée dans des matrices différentes par d'autres auteurs.

Avec l'expansion du champ d'application des isotopes du mercure, les techniques d'introduction développées pour l'analyse de la spéciation des formes moléculaires du mercure prennent une place grandissante dans l'analyse isotopique (ex: chromatographie en phase gazeuse couplée au MC-ICP-MS). D'autre part, d'autres techniques de préconcentration du mercure pour des échantillons faiblement concentrés ou de séparation de la matrice par des colonnes chromatographiques ont été développées. Associées à ces techniques d'introduction, les techniques de mesure de la composition isotopique par double spike ont fait leur apparition. Il est donc indispensable de poursuivre la caractérisation de matériaux de référence permettant l'intercomparaison entre les nouvelles méthodes et la méthode conventionnelle d'analyse utilisée dans cette étude.

- Détermination de l'amplitude des fractionnements isotopiques sur les isotopes du mercure dans des processus physiques et chimiques.

Afin d'interpréter les variations de composition isotopique du mercure dans l'environnement, il est essentiel de caractériser les réactions susceptibles de fractionner les isotopes du mercure. Dans ce travail, nous nous sommes d'abord intéressés à caractériser le fractionnement isotopique du mercure lors de son évaporation dans le système liquide-vapeur. Ensuite, nous avons étudié la réaction de réduction du Hg(II) en Hg(0) par un agent abiotique d'intérêt biogéochimique: les rouilles vertes.

Le système liquide-vapeur étudié représente une transformation physique dans laquelle

le mercure subit un changement de phase (liquide-gaz) à l'équilibre ou bien en cinétique. On peut trouver ce type de réaction dans les systèmes industriels par exemple lors de distillations ou bien dans les systèmes géologiques comme les gisements des ceintures mercurifères. D'un point de vue géochimique, ce changement de phase est très intéressant et a été étudié dans de nombreux autres systèmes isotopiques dont les applications principales sont orientées vers la compréhension de la formation du système solaire (évaporation/condensation des éléments dans les météorites).

L'amplitude attendue des fractionnements isotopiques dans un système évaporant en cinétique dépend en première approximation de la racine carrée du rapport des masses. La composition isotopique du mercure évaporé était donc supposée être fractionnée par rapport au liquide initial de plus de 10‰ pour le rapport $^{202}/^{198}\text{Hg}$. Les résultats de cette étude ont montré que l'évaporation du mercure liquide en cinétique présentait un facteur de fractionnement de l'ordre de 6.7‰ (exprimé en $^{202}\Delta_{(\text{liq-gaz})}$) entre le liquide et la vapeur, confirmant ainsi un fractionnement isotopique de grande ampleur. Le facteur de fractionnement mesuré diffère néanmoins significativement du facteur de fractionnement théorique comme reporté auparavant sur d'autres systèmes isotopiques. Néanmoins, cette réaction est pour l'instant la seule à avoir montré des fractionnements isotopiques dépendants de la masse d'une si grande amplitude. L'effet de la température lors de l'évaporation en cinétique a mis en évidence que le facteur de fractionnement diminuait considérablement avec celle-ci, contrairement à la théorie où le fractionnement cinétique est considéré comme indépendant de la température. Ces résultats ont été décrits par un modèle conceptuel dans lequel une augmentation des échanges à l'interface entre le liquide et la vapeur est responsable de la diminution de l'amplitude des fractionnements isotopiques. D'un autre côté, le facteur de fractionnement mesuré lors de l'évaporation à l'équilibre, avec une valeur de $^{202}\Delta_{(\text{liq-gaz})}$ de l'ordre de 0.86‰, contraste largement avec l'évaporation en cinétique et permet ainsi l'identification du type de fractionnement dans un système où l'évaporation est susceptible de se produire.

Ce travail a aussi révélé des fractionnements indépendants de la masse sur les isotopes du mercure lors de l'évaporation à l'équilibre ainsi qu'en cinétique. Basé sur les travaux théoriques de Schauble et Bigeleisen, le type de fractionnement indépendant de la masse mis en évidence a été attribué au «nuclear field shift effect» qui n'avait alors été entrevu que théoriquement. Ce type de fractionnement indépendant de la masse n'est susceptible de se produire que lors de changements d'états d'oxydations entre le produit et le réactif. Dans la réaction entre le mercure liquide et le mercure gazeux à l'équilibre, il n'y a à priori pas de changement d'état d'oxydation. Néanmoins, les phases condensées comme le liquide effectuent un partage des électrons externes afin de maintenir la cohésion et donc diminuent l'état d'oxydation apparent du mercure dans le liquide par rapport au gaz. Ces réflexions ont été confirmées par des calculs de fractionnement isotopique entre le liquide et la vapeur à

Conclusion

l'équilibre menés par Edwin Schuble suivant la méthodologie développée dans son article de 2007. La figure ci-dessous présente la variation de composition isotopique entre le liquide et la vapeur ($1000\ln\beta_{202-198} = ^{202}\Delta_{\text{liq-vapeur}}$) en fonction de la température. Cette modélisation est issue d'une communication personnelle avec Edwin Schuble à la suite de la présentation de ces travaux à la conférence internationale Goldschmidt 2007 (Köln, Allemagne).

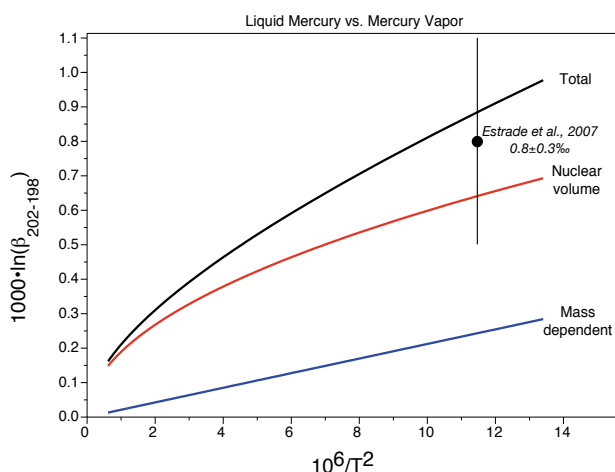


Figure 1 : Modélisation du fractionnement isotopique pour l'équilibre liquide-vapeur sur le rapport $^{202/198}\text{Hg}$ en fonction de $10^6/T^2$ (T en Kelvin). (Communication personnelle E. Schuble, 2007)

Schauble indiquait que dans l'équilibre liquide-vapeur, la proportion de «nuclear field shift effect» représentait 70% du fractionnement total, le reste étant issu de fractionnement dépendant de la masse. De notre côté, en utilisant les différents couples isotopiques du mercure, nos calculs indiquaient $85 \pm 15\%$ de «nuclear field shift effect», en accord avec les modélisations de Schuble. Ces résultats n'ont pas pu être reportés dans l'article car les incertitudes sur le calcul des proportions ont été considérées trop importantes au vu de l'ampleur du fractionnement indépendant de la masse.

Le travail mené sur la réduction du Hg(II) en Hg(0) a été réalisé en utilisant les rouilles vertes afin de déterminer l'amplitude du fractionnement isotopique lors d'une réduction par un agent réducteur abiotique. Les rouilles vertes sont de puissants réducteurs des métaux que l'on retrouve dans des milieux anoxiques comme dans certains sols ou dans les eaux souterraines. Le protocole expérimental mis en place dans cette étude n'a pas permis d'observer strictement la réduction du Hg(II) par les rouilles vertes. La réaction de la rouille verte avec le mercure étant documentée pour être très rapide, nous avons choisi d'arrêter l'avancement de la réaction en oxydant la rouille verte par l'introduction de Hg(II) en solution dans l'acide nitrique. Néanmoins, cette oxydation a conduit à la formation de sous produits de la rouille verte. Ces différentes phases ont pu être identifiées par microscopie électronique à transmission révélant entre autre de la magnétite, capable de réduire le Hg(II) en solution. Ces résultats indiquaient que la fraction de mercure échantillonnée en fonction du temps pouvait être non-représentative de la fraction résiduelle de Hg(II) restant en solution. Dans ce cas, il a été difficile d'établir un système de Rayleigh dans lequel le facteur

de fractionnement est déterminé à partir de la mesure de la composition isotopique de la fraction de mercure restant dans la solution. Néanmoins, les expériences ayant conduit à une réduction quasi-totale du Hg(II) ont révélé de précieuses informations. L'analyse de la composition isotopique pour ces fractions considérées comme des fractions résiduelles de Hg(II) a montré des compositions isotopiques enrichies en isotopes légers suggérant que le Hg(0) produit par la réaction de réduction avait été piégé par les phases solides en solutions. L'analyse de ces phases par microscopie électronique à transmission a permis de confirmer cette hypothèse en révélant des gouttelettes de Hg(0) piégées. À partir de ces fractions, il a ainsi été possible de déterminer un facteur de fractionnement minimum pour la réduction du Hg(II) par un réducteur abiotique. Le facteur de fractionnement déterminé est au minimum de 1.3 ‰ ($^{202}\Delta_{\text{Hg(II)-Hg(0)}}$) et le fractionnement isotopique dépend de la masse. Ces résultats sont dans la gamme de fractionnement isotopique déterminée pour la réduction bactérienne en utilisant des réducteurs comme SnCl₂ ou NaBH₄. Cette étude sur les rouilles vertes, a permis l'investigation d'un système complexe faisant intervenir une réduction par l'intermédiaire du Fe(II) et dans lequel du mercure en phases liquide, solide et gazeuse coexiste, simulant ainsi un système naturel et rendant l'exploitation de sa composition isotopique difficile.

Néanmoins, ces résultats sur les rouilles vertes viennent confirmer que l'amplitude de fractionnement des isotopes du mercure dans un système soumis à la réduction est relativement faible ($^{202}\Delta_{\text{Hg(II)-Hg(0)}}$ = 2‰ au maximum). Plus généralement, la réduction est une réaction clé de la mobilité du mercure dans les compartiments terrestres. Ainsi, des variations de compositions isotopiques significatives dans le réservoir contenant le Hg(II) ne peuvent intervenir que si la fraction de mercure qui est réduite est importante. Il est donc suggéré que des fractionnements isotopiques liés à la réduction ne pourront être enregistrés que dans des environnements spécifiques où les contraintes physico-chimiques sont suffisantes pour réduire d'importantes quantités de mercure. Ceci implique que l'apport de mercure extérieur à un système, avec une composition isotopique suffisamment fractionnée par rapport au mercure présent initialement, est susceptible de conserver sa signature isotopique initiale.

La détermination des facteurs de fractionnements sur les isotopes du mercure a surtout été focalisée sur la photoréduction du Hg(II) en Hg(0) dans les systèmes aquatiques. En effet, ce type de réaction est une des sources d'émission importante du mercure dans l'atmosphère et contribue pour une grande part au budget de mercure introduit le long de la chaîne trophique. Dans ces réactions, des fractionnements isotopiques indépendants de la masse ont été mis en évidence, attribués principalement au «magnetic isotope effect». Les fractionnements indépendants de la masse lors de la photoréduction engendrent des anomalies positives sur les $\Delta^{199}\text{Hg}$ et $\Delta^{201}\text{Hg}$ pour le Hg(II) en solution et sont contrebalancés par des anomalies négatives pour le Hg(0) émis à l'atmosphère. Néanmoins de récents travaux ont montré qu'en utilisant des médiateurs organiques contenant des composés soufrés, le

sens du fractionnement isotopique indépendant de la masse pouvait être inversé et que la photoréduction pouvait également engendrer du «nuclear field shift effect». Ces résultats sont autant d'indices pour interpréter les variations de compositions isotopiques dans les systèmes aquatiques. L'atmosphère est le compartiment de transport du mercure à longue distance dans lequel de nombreuses réactions chimiques et photochimiques interviennent pour déposer le mercure dans les écosystèmes. Il n'existe à l'heure actuelle aucune expérimentation sur les réactions responsables de la déposition (ex: oxydation du Hg(0) par les halogènes, Br et Cl). Afin d'entrevoir la compréhension du cycle biogéochimique du mercure, il faut donc focaliser les prochains travaux expérimentaux sur la mesure des fractionnements isotopiques lors de l'oxydation du mercure élémentaire.

- Utilisation des isotopes du mercure appliquée à la discrimination et au traçage des sources anthropiques dans l'environnement.

Le mercure émis dans l'atmosphère par les sources anthropiques provient essentiellement des compartiments géologiques. La documentation des variations de composition isotopique de ces environnements a révélé une large gamme de fractionnements dépendants de la masse associée à de faibles fractionnements indépendants de la masse. Dans ce travail, nous nous sommes basés sur l'hypothèse que les sources d'émission anthropique du mercure dans l'atmosphère ne présentaient que peu ou pas de fractionnement indépendant de la masse. L'analyse de la composition isotopique des lichens a révélé des fractionnements indépendants de la masse négatifs sur les $\Delta^{199}\text{Hg}$ et $\Delta^{201}\text{Hg}$ attribués au «magnetic isotope effect». Les lichens étant considérés comme des échantillonneurs de la matière atmosphérique, il a été suggéré que le Hg de l'atmosphère contenait ces anomalies de fractionnement isotopique. La photoréduction du mercure aquatique produisant des anomalies négatives pour le Hg(0) émis à l'atmosphère, nous avons suggéré que l'atmosphère était le réservoir complémentaire du compartiment aquatique en terme d'anomalies isotopiques. Néanmoins, la gamme de variations des anomalies mesurées dans des lichens situés à plusieurs endroits du globe indiquait qu'elles ne pouvaient pas uniquement provenir de la photoréduction du mercure aquatique. La composition isotopique a été interprétée dans une première approche comme un mélange entre le réservoir atmosphérique global et les sources anthropiques ne possédant que peu ou pas d'anomalie. Néanmoins, tout bilan est difficile à mettre en place car le mercure anthropique émis ne possédant pas d'anomalie isotopique peut en développer au cours de sa vie dans le cycle biogéochimique avant d'être réémis dans l'atmosphère.

Dans l'étude de la composition isotopique des lichens de la région de Metz, nous avons pu mettre en évidence que l'anomalie enregistrée par le lichen est caractéristique de la zone

d'échantillonnage de ce lichen. Ainsi, dans les zones où l'impact anthropique est le plus fort, les lichens présentent les plus faibles anomalies isotopiques. Ces résultats ont été interprétés en termes de mélange de sources dans lequel le lichen échantillonne le mercure provenant du réservoir global d'un côté (avec des anomalies isotopiques négatives) et, de l'autre, les sources anthropiques directes qui ne contiennent pas d'anomalies. Ce modèle simple est basé sur l'hypothèse que le transport du Hg dans l'atmosphère et la déposition dans le lichen n'engendrent pas de fractionnement isotopique. Comme énoncé précédemment, il est nécessaire de mener des expérimentations afin de déterminer si l'oxydation atmosphérique engendre un fractionnement isotopique ou non, s'il peut être accompagné de fractionnements indépendants de la masse et si oui, de quelle amplitude. L'analyse des compositions isotopiques dans différents lichens en fonction de l'espèce et de l'année d'échantillonnage suggère qu'aucun fractionnement isotopique significatif ne modifie la composition isotopique du mercure dérivé de l'atmosphère. Pour donner suite à ces travaux, il reste nécessaire d'étudier expérimentalement l'incorporation du mercure par le lichen afin de déterminer s'il existe aussi des fractionnements isotopiques associés.

De plus, des fractionnements isotopiques indépendants de la masse privilégiant le ^{201}Hg par rapport au ^{199}Hg ont été mesurés dans les lichens de la zone urbaine et peuvent entre autre être interprétés par des mélanges de processus dans l'atmosphère. Ce type de fractionnement contraste avec tous les autres travaux expérimentaux et théoriques reportant des enrichissements plus important en ^{199}Hg qu'en ^{201}Hg et indique qu'il reste de nombreux travaux à réaliser d'un point de vue expérimental mais aussi théorique. À l'heure actuelle, seul un travail théorique sur le «nuclear field shift effect» a été réalisé. Les géochimistes des isotopes du mercure doivent donc travailler de concert avec des théoriciens afin de percer les secrets des nombreux modes de fractionnements indépendants de la masse.

La combinaison des fractionnements isotopiques dépendants et indépendants de la masse ont permis de discriminer les sources anthropiques d'émissions atmosphériques du mercure dans l'agglomération de Metz, montrant des contrastes significatifs entre les sources dans les zones urbaines et les zones industrielles. Ils ont permis de tracer le mercure émis des sources industrielles dans la vallée réceptrice de ces émissions. De plus, ils ont rendu possible le traçage du mercure émis en zone urbaine dans les zones périurbaines et rurales. Néanmoins, il n'a pas été possible de déterminer précisément la contribution de la source anthropique par rapport au mercure atmosphérique global, car ce réservoir est pour l'instant mal caractérisé. De nombreux travaux restent à faire pour déterminer précisément la composition isotopique de l'atmosphère à différentes échelles. Ces travaux ont mis en évidence que l'atmosphère, même si elle est globalement homogène du point de vue de sa concentration, ne l'est sûrement pas du point de vue de sa composition isotopique.

L'analyse de la composition isotopique dans les sols contaminés par la fonderie Pb-Zn de Metaleurop a montré clairement que le mercure était issu d'un mélange entre un pôle de contamination et le mercure du fond géogénique. Dans ces sols, aucun fractionnement isotopique indépendant de la masse significatif n'a été mesuré. Dans ce «cas d'école», l'analyse de la composition isotopique des poussières émises à la cheminée a montré que la fonderie était bien à l'origine de cette contamination. De plus, les relations mises en évidence entre la composition isotopique et la concentration en mercure ont montré que la signature isotopique de la source de contamination est conservée avec le temps et les conditions physico-chimiques du sol. Ainsi, les processus menant à la mobilité ou à l'évasion du mercure du sol ne se sont pas produits dans une proportion assez importante pour altérer cette signature. Néanmoins, n'ayant pas mesuré la signature isotopique exacte du fond géochimique, nous n'avons pas déterminé la contribution de la fonderie dans les sols en fonction de la distance.

L'étude de la composition isotopique dans les sols de Metz a été réalisée dans un contexte urbain. De nombreuses sources anthropiques ont pu être mélangées, participant aux teneurs élevées en mercure de certains sols de la zone d'étude. Cette zone contient une centrale de combustion de charbon et un incinérateur, qui peuvent être des sources importantes de mercure. La centrale de combustion de charbon est en activité depuis le début des années 60. En 1992, elle s'est équipée de turbines à gaz et le charbon ne représente plus que 10% de la production actuelle d'électricité. Aucune donnée sur ses émissions de mercure ne nous a été fournie. D'un autre côté, un premier incinérateur avait été construit en 1969 sur le site de l'actuel. Avant sa fermeture en 1997, la concentration des émissions en mercure en sortie de cheminée était de l'ordre de $100 \mu\text{g.Nm}^{-3}$ (concentrations élevées, mais en dessous des normes d'émissions en vigueur à l'époque). Un nouvel incinérateur équipé des meilleures technologies disponibles pour l'épuration des fumées a été mis en service en 2001.

La composition isotopique du mercure dans les sols de l'agglomération de Metz a révélé un mélange entre un pôle de contamination anthropique et le mercure du fond géogénique. Des fractionnements indépendants de la masse de très faible amplitude ont été mis en évidence uniquement dans les sols les plus faiblement concentrés. Comme dans le premier cas d'étude, nous montrons ici que la composition isotopique du mercure est préservée avec le temps et les conditions du sol. Ayant mesuré la composition isotopique du fond géochimique, nous avons déterminé précisément la contribution de la source de contamination dans chacun des sols de la zone étudiée. Les sols fortement impactés par la source anthropique présentaient une dispersion restreinte autour de la zone de l'incinérateur et de la centrale de combustion de charbon, pointant ces deux sources comme des contributeurs potentiels de contamination. Au regard de la littérature, les charbons ont une valeur moyenne de $\delta^{202}\text{Hg}$ de l'ordre de -1‰ significativement différente de la signature isotopique

du pôle de contamination. D'autre part, les centrales de combustion de charbon émettent principalement du Hg⁰ alimentant majoritairement le réservoir atmosphérique. Assumant qu'aucun fractionnement entre le charbon et les émissions de la centrale de combustion ne s'est produit, la centrale de charbon n'est probablement pas la source anthropique ayant engendrée les teneurs élevées en mercure dans les sols.

Du point de vue de l'incinérateur, des résultats préliminaires sont présentés succinctement en annexe 2. Les concentrations en mercure mesurées dans les émissions sont actuellement de l'ordre de 2 µg.Nm⁻³ (en dessous des normes en vigueur: 50 µg.Nm⁻³), soit environ 50 fois plus faibles que l'ancien incinérateur. Le Hg(II) est la forme chimique la plus représentée dans les émissions de mercure (61% pour Hg(II) contre 39% pour Hg⁰), en accord avec la littérature. L'étude de la composition isotopique des cendres à l'intérieur de l'incinérateur indique que le mercure est soumis entre autre à des processus de condensation physique. La composition isotopique sur les trois campagnes de mesure menées sur plusieurs années indique une valeur $\delta^{202}\text{Hg}$ moyenne pour les déchets entrant de -0.58‰ sans fractionnement indépendant de la masse, représentatif des grands gisements de mercure. L'investigation de la composition isotopique du mercure en sortie de cheminée en fonction de sa spéciation sur trois campagnes de mesure en 2009 permet de fournir des éléments intéressants du point de vue de la signature des émissions de ce type de système industriel. Aucun fractionnement indépendant de la masse n'a été mesuré sur le Hg(II) émis, susceptible de se déposer à proximité de l'incinérateur. De plus, la composition isotopique moyenne du Hg(II) émis est de l'ordre de 0.1‰. Cette valeur coïncide avec la valeur de la source de contamination révélée par l'étude de la composition isotopique des sols à proximité de l'incinérateur. Ainsi, en admettant que la composition isotopique des déchets et celle du Hg(II) en sortie de cheminée n'ont pas varié au cours du temps entre les deux incinérateurs, l'ancien incinérateur est vraisemblablement à l'origine de la contamination en mercure mesurée dans les sols. Cette étude ouvre aussi de nombreuses perspectives sur la compréhension des réactions mises en jeu dans les processus de combustion. Par exemple, des fractionnements isotopiques indépendants de la masse ont été mesurés sur le Hg⁰ émis, et sont certainement représentatifs de la qualité de la combustion et/ou du fonctionnement des systèmes d'épurations des fumées. Cependant, ces fractionnements indépendants de la masse attribués au «magnetic isotope effect» ont été créés à l'intérieur de l'incinérateur sans intervention de processus photochimiques. Une nouvelle fois, ces résultats montrent à quel point il est nécessaire de caractériser expérimentalement et théoriquement les différents types de fractionnements indépendants de la masse du mercure.

Plus généralement, dans ce travail, nous avons mesuré la composition isotopique de deux systèmes anthropiques. Nous avons discriminé des sources anthropiques du fond géochimique. Nous avons tracé des émissions des émissions anthropiques à une échelle de

Conclusion

quelques kilomètres carrés dans des sols. À une échelle de plusieurs centaines de kilomètres carrés, nous avons utilisé la composition isotopique des lichens pour discriminer les sources anthropiques directes du réservoir atmosphérique. Nous pouvons de plus entrevoir que les isotopes du mercure pourront un jour tracer les sources anthropiques à une échelle globale. Ce travail pose les bases du traçage des pollutions en utilisant les isotopes du mercure comme traceur de ses émissions et ouvre de nombreuses perspectives à explorer et notamment sur les phénomènes de déposition du mercure atmosphérique. D'autre part, l'investigation de la composition isotopique dans les systèmes industriels doit être un axe à développer afin d'étudier les processus réactionnels et de déterminer l'influence des procédés de combustion et d'épuration sur la composition isotopique des formes de mercure émises à l'atmosphère. Dans tous les cas, la méthodologie mise en oeuvre dans cette thèse pourra être utilisée pour une application à la discrimination et au traçage de nombreuses autres sources de pollutions.